Table 2 Genotypic characteristics of the subjects

SNP ID	*CHR*	*Position (Build 36.3)*	*Nearby gene*	*Allele 1/2*	*BP-associated allele*	*Genotype*	*HWE P-value*
rs16998073	4	81 403 365	*FGF5*	T/A	T	120/514/644	0.24
rs11014166	10	18 748 804	*CACNB2*	T/A	A	4/124/1151	0.73
rs1530440	10	63 194 597	*C10orf107*	T/C	C	30/296/953	0.22
rs1004467	10	104 584 497	*CYP17A1*	A/G	A	559/567/153	0.62
rs11191548	10	104 836 168	*NT5C2*	T/C	T	675/504/100	0.66
rs381815	11	16 858 844	*PLEKHA7*	C/T	T	842/381/56	0.13
rs2681472	12	88 533 090	*ATP2B1*	A/G	A	546/562/171	0.17
rs2681492	12	88 537 220	*ATP2B1*	C/T	T	168/561/549	0.19
rs6495112	15	72 619 851	*ARID3B*	A/C	A	530/575/173	0.39
rs1378942	15	72 864 420	*CSK*	A/C	C	49/410/817	0.78
rs12946454	17	40 563 647	*PLCD3*	T/A	T	34/343/901	0.84
rs16948048	17	44 795 465	*ZNF652*	G/A	G	18/326/935	0.08

Abbreviations: BP, blood pressure; CHR, chromosome; HWE, Hardy–Weinberg equilibrium.

Table 3 Mean BMI, VFA and SFA for 12 blood pressure risk variants

		Mean ± s.d.								
		BMI (kg m^{-2})			*VFA (cm^2)*			*SFA (cm^2)*		
		Genotype			*Genotype*			*Genotype*		
SNP ID	*Nearby gene*	*11*	*12*	*22*	*11*	*12*	*22*	*11*	*12*	*22*
rs16998073	*FGF5*	28.8 ± 4.7	29.0 ± 5.8	29.0 ± 6.0	126.2 ± 66.1	121.6 ± 66.5	125.3 ± 65.9	227.4 ± 98.3	224.5 ± 111.0	227.7 ± 98.7
rs11014166	*CACNB2*	27.0 ± 2.7	29.6 ± 6.1	28.9 ± 5.8	123.4 ± 82.2	136.7 ± 68.2	122.5 ± 65.8	178.6 ± 35.8	233.7 ± 106.4	225.8 ± 103.6
rs1530440	*C10orf107*	30.8 ± 6.5	28.6 ± 5.4	29.1 ± 5.9	129.8 ± 63.1	120.2 ± 66.4	124.9 ± 66.2	236.4 ± 119.2	223.0 ± 91.4	227.2 ± 106.9
rs1004467	*CYP17A1*	28.4 ± 5.6	29.5 ± 6.1	29.4 ± 5.2	117.5 ± 64.9	130.6 ± 68.5	122.5 ± 59.3	215.5 ± 92.7	231.4 ± 111.5	247.9 ± 107.9
rs11191548	*NT5C2*	28.6 ± 5.8	29.5 ± 5.9	28.9 ± 5.1	119.2 ± 65.3	130.9 ± 68.6	120.5 ± 55.7	217.2 ± 96.0	238.5 ± 113.2	228.1 ± 98.8
rs381815	*PLEKHA7*	29.2 ± 5.9	28.7 ± 5.7	27.8 ± 4.3	124.1 ± 64.2	124.3 ± 71.5	117.9 ± 55.9	229.4 ± 105.9	221.5 ± 101.6	215.3 ± 83.1
rs2681472	*ATP2B1*	29.2 ± 5.8	28.8 ± 5.4	29.0 ± 7.0	127.1 ± 67.5	121.5 ± 64.8	121.8 ± 65.8	227.4 ± 100.4	223.5 ± 100.3	233.1 ± 123.6
rs2681492	*ATP2B1*	29.0 ± 7.1	28.7 ± 5.2	29.3 ± 5.9	121.9 ± 66.3	121.4 ± 64.8	127.0 ± 67.4	234.6 ± 123.9	221.9 ± 98.3	228.7 ± 102.3
rs6495112	*ARID3B*	28.9 ± 5.8	29.0 ± 5.7	29.3 ± 6.2	122.5 ± 63.4	125.0 ± 69.2	124.9 ± 64.3	223.7 ± 106.5	229.5 ± 102.6	225.1 ± 99.2
rs1378942	*CSK*	28.0 ± 4.2	28.9 ± 6.1	29.1 ± 5.7	110.0 ± 63.3	121.8 ± 62.4	125.6 ± 67.6	222.9 ± 84.5	225.9 ± 104.3	227.0 ± 104.7
rs12946454	*PLCD3*	30.1 ± 8.2	28.6 ± 5.0	29.1 ± 5.9	137.2 ± 80.0	123.0 ± 67.4	123.7 ± 65.1	254.4 ± 105.0	216.4 ± 93.7	229.2 ± 107.0
rs16948048	*ZNF652*	28.1 ± 2.8	29.4 ± 5.9	28.9 ± 5.8	128.6 ± 73.7	124.8 ± 65.9	123.5 ± 66.1	215.0 ± 60.6	227.0 ± 96.3	226.5 ± 106.9

Abbreviations: BMI, body mass index; SFA, subcutaneous fat area; SNP, single nucleotide polymorphism; VFA, visceral fat area.
11, allele1/allele1; 12, allele1/allele2; 22, allele2/allele2. Allele 1 and allele 2 of each SNP is indicated in Table 2.

in the *CYP17A1* gene was significantly associated with reduced BMI (P=0.0018). The other SNPs were not significantly associated with BMI. No SNP was significantly associated with VFA. The A-allele of rs1004467 in the *CYP17A1* and the T-allele of rs11191548 in the *NT5C2* gene were significantly associated with reduced SFA. These SNPs are in linkage disequilibrium, as reported in the HapMap database (D'=0.98, r^2=0.71), and the A-allele of rs1004467 and T-allele of rs11191548 are reported to be risk alleles for increased blood pressure.[20,21]

BMI, VFA and SFA are known to be affected by gender; therefore, we compared rs1004467 and rs11191548 alleles with anthropometric parameters (BMI, VFA and SFA) in men and women independently (Table 5). Associations of both SNPs with VFA (P=0.0018 and P=0.0043) and SFA (P=0.00039 and P=0.0021) in women were significant, except the association of T-allele of rs11191548 with VFA. The VFA and SFA values of the rs11191548 genotype suggest that the recessive model would be the best-fitted model both in men and women. By using the recessive model, results revealed significant associations of the rs11191548 genotype with VFA (P=0.0022) and SFA in women (P=0.00059). These SNPs did not show any association with VFA or SFA in men, suggesting that they exhibit sexual dimorphism, as has been suggested in a recent report.[26] As both rs1004467 and rs11191548 were associated with a reduction in both VFA and SFA, we examined the association of these SNPs with total fat area. The SNPs were significantly associated with total fat area (P=0.00012 at rs1004467, P=0.00052 at rs11191548 in additive model) in women, but not in men, suggesting that risk allele for high blood pressure of these SNPs are associated with reduced adiposity in women. The very small mean F_{ST} value (0.00023) indicated no population structure in our subjects. As we collected the samples from nine institutes in four regions of Japan (Supplementary Table 1), we tested multiple linear regression analysis with age and institute as explanatory variables in men and women. Very similar results were observed. In additive model, significant associations of the

Table 4 Relationship between blood pressure-associated loci and adiposity measures

		BMI			*VFA*			*SFA*		
SNP ID	*Nearby gene*	β	*s.e.*	P-*value*	β	*s.e.*	P-*value*	β	*s.e.*	P-*value*
rs16998073	*FGF5*	−0.002	0.003	0.55	−0.003	0.010	0.78	−0.010	0.008	0.22
rs11014166	*CACNB2*	−0.005	0.007	0.48	−0.043	0.021	0.043	−0.008	0.017	0.63
rs1530440	*C10orf107*	−0.002	0.004	0.71	0.010	0.014	0.48	−0.005	0.011	0.64
rs1004467	*CYP17A1*	−0.010	0.003	**0.0018**	−0.022	0.010	0.027	−0.030	0.008	**0.00011**
rs11191548	*NT5C2*	−0.008	0.003	0.015	−0.019	0.011	0.078	−0.026	0.008	**0.0016**
rs381815	*PLEKHA7*	−0.007	0.004	0.046	−0.004	0.012	0.76	−0.015	0.009	0.10
rs2681472	*ATP2B1*	0.002	0.003	0.43	0.006	0.010	0.52	0.005	0.008	0.49
rs2681492	*ATP2B1*	0.003	0.003	0.34	0.006	0.010	0.54	0.006	0.008	0.40
rs6495112	*ARID3B*	−0.002	0.003	0.45	−0.004	0.010	0.65	−0.007	0.008	0.36
rs1378942	*CSK*	0.005	0.004	0.20	0.010	0.012	0.40	0.005	0.009	0.61
rs12946454	*PLCD3*	−0.003	0.004	0.39	0.009	0.013	0.50	−0.011	0.010	0.28
rs16948048	*ZNF652*	0.005	0.004	0.30	0.008	0.014	0.57	0.005	0.011	0.67

Abbreviations: BMI, body mass index; SFA, subcutaneous fat area; SNP, single nucleotide polymorphism; VFA, visceral fat area.
Data were derived from a linear regression analysis. The values of BMI, VFA and SFA were logarithmically transformed. Logarithmically transformed BMI, VFA and SFA were adjusted for age and gender. Tested alleles are risk alleles of increased blood pressure.

Table 5 Relationship between rs1004467 and rs11191548, and adiposity in men and women

			Values at each genotype			*Additive model*		*Recessive model*	
SNP ID (gene)	*Phenotype*	*Gender*	*11*	*12*	*22*	β *(s.e.)*	P-*value*	β *(s.e.)*	P-*value*
rs1004467	*n*	Men	233	259	64				
(*CYP17A1*)		Women	326	308	89				
	BMI ($kg\,m^{-2}$)	Men	29.7±6.6	30.6±5.9	30.1±5.1	−0.011 (0.005)	0.029	−0.017 (0.006)	0.0085
		Women	27.6±4.6	28.5±6.0	28.9±5.3	−0.010 (0.004)	0..017	−0.013 (0.006)	0.019
	VFA (cm^2)	Men	152.9±67.7	160.6±69.2	142.8±59.9	0.004 (0.014)	0.78	−0.012 (0.019)	0.52
		Women	92.3±49.2	105.4±56.8	107.8±54.7	−0.044 (0.014)	**0.0018**	−0.061 (0.019)	**0.0014**
	SFA (cm^2)	Men	198.6±103.0	211.9±113.8	215.4±106.7	−0.028 (0.013)	0.037	−0.036 (0.018)	0.047
		Women	227.6±82.7	248.0±106.9	271.2±103.3	−0.033 (0.009)	**0.00039**	−0.040 (0.013)	**0.0020**
rs11191548	*n*	Men	289	220	47				
(*NT5C2*)		Women	386	284	53				
	BMI ($kg\,m^{-2}$)	Men	30.0±6.8	30.6±5.4	29.4±5.4	−0.007 (0.005)	0.19	−0.013 (0.006)	0.049
		Women	27.6±4.7	28.7±6.1	28.5±4.8	−0.010 (0.004)	0.021	−0.015 (0.006)	0.0080
	VFA (cm^2)	Men	153.8±68.0	161.3±69.3	137.2±54.8	0.007 (0.014)	0.65	−0.008 (0.018)	0.65
		Women	93.3±49.3	107.4±58.1	105.8±52.8	−0.043 (0.015)	0.0043	−0.059 (0.019)	**0.0022**
	SFA (cm^2)	Men	202.1±107.5	214.3±111.3	199.9±102.5	−0.023 (0.014)	0.10	−0.035 (0.018)	0.048
		Women	228.5±84.9	257.4±111.1	253.0±89.0	−0.031 (0.010)	**0.0021**	−0.044 (0.013)	**0.00059**

Abbreviations: BMI, body mass index; SFA, subcutaneous fat area; SNP, single nucleotide polymorphism; VFA, visceral fat area.
Values are shown as the mean±s.d. Data were derived from a linear regression analysis. The values of BMI, VFA and SFA were logarithmically transformed. Logarithmically transformed BMI, VFA and SFA were adjusted for age. Tested alleles (allele1 at both SNPs) are risk alleles of increased blood pressure.

rs1004467 and rs11191548 genotype with VFA (P=0.0015 and 0.0011, respectively) and SFA (P=0.00021 and 0.00062, respectively) were observed in women (Supplementary Table 2). Statistical analysis using analysis of covariance indicated significant associations of the rs1004467 and rs11191548 genotype with VFA (P=0.0020 and 0.0015, respectively) and SFA (P=0.00033 and 0.00042, respectively) in women (Supplementary Table 2). As some diabetes medications have an effect on adiposity,[27] we performed the analysis excluding 147 type 2 diabetic patients treated with sulfonylureas, biguanides and thiazolidinediones We found the similar significant associations of the rs1004467 and rs11191548 genotype with VFA and SFA in women (Supplementary Table 3).

We have reported that rs1558902 in the *FTO* gene is associated with both VFA and SFA,[11] and that rs7498665 in the *SH2B1* gene is associated with VFA.[17] Thus, we examined SNP×SNP epistasis in men, women and all subjects. The combination of rs1004467 and rs7498665 exhibited no epistatic effect on VFA in men (P=0.43), women (P=0.86) or all subjects (P=0.76). The combination of rs1004467 and rs1558902 did not show epistatic effect on VFA in men (P=0.99), women (P=0.53) or all subjects (P=0.60), or on SFA in men (P=0.63), women (P=0.83) or all subjects (P=0.89).

Among the SNPs tested in this study, rs16998073 in the *FGF5* gene and rs11191548 in the *NT5C2* gene were associated with increased systolic blood pressure ($P<0.05$). Rs11191548 in the *NT5C2* gene were also associated with hypertension ($P<0.05$). We could replicate the association between blood pressure and the above two SNPs that were reported to be strongly associated with blood pressure in the Japanese population (Supplementary Table 4).[28]

DISCUSSION

In this study, we showed that the A-allele of rs1004467 in the *CYP17A1* and the T-allele of rs11191548 in the *NT5C2* gene were significantly associated with reduced VFA, SFA and total fat area in women. Association of T-allele of rs11191548 in the *NT5C2* gene with increased systolic blood pressure and hypertension was replicated in our sample, as reported previously.[28] Our hypothesis was that these risk alleles would be associated with increased VFA and/or SFA as increased adiposity is a risk for hypertension;[4,5] however, these alleles affected decreased adiposity. The associations between SNPs and increased blood pressure/hypertension were evaluated after being adjusted for BMI, age and gender. Thus, the SNPs associated with visceral fat obesity-related and gender-dependent hypertension would be excluded in the screening stage. Indeed, recent analysis has shown that genetic variation near insulin receptor substrate 1 (*IRS1*) is associated with reduced adiposity and an impaired metabolic profile.[29] Thus, it is likely that rs1004467 and rs11191548 are associated with reduced VFA and SFA, as well as with hypertension in women.

The SNPs rs1004467 and rs11191548 were not associated with BMI in men or women, as reported for rs2943650 near *IRS1*.[29] As BMI represents both fat and lean body mass, our observation suggests that these SNPs influence a reduction in VFA and SFA, or influence an increased percentage of lean body mass. The significant associations of rs1004467 and rs1191548 with reduced VFA and SFA were observed in women, but not in men. The rs1004467 SNP is located in the intron of the *CYP17A1* gene. CYP17A1 is involved in the biosynthesis of glucocorticoids, mineral corticoids, androgens and estrogens.[30] The rs1004467 risk allele may reflect differences in *CYP17A1* gene expression that alter the biosynthesis of steroid hormones, leading to hypertension and reduced adiposity in women. The region of linkage disequilibrium that includes rs1004467 and rs11191548 contains a couple of genes in addition to *CYP17A1*: *NT5C2*, arsenic (+3 oxidation state) methyltransferase (*AS3MT*) and cyclin M2 (*CNNM2*). NT5C2 is a cytosolic IMP/GMP selective 5′-nucleotidase and involved in nucleic acids or DNA synthesis.[31] CNNM2 (ancient conserved domain protein, ACDP2) is a transporter of magnesium, which is required for the catalytic activity of numerous metalloenzymes.[32] Thus, these genes would be important for metabolism in adipocyte hyperplasia and hypertrophy. Further investigation is warranted to elucidate the functional SNPs and susceptibility genes.

We have previously reported that *FTO* rs1558902 is associated with VFA and SFA, and that *SH2B1* rs7498665 is associated with VFA.[11,17] Epistasis, or gene–gene interaction, has recently received much attention in human genetics.[33] In this study, the effect of these SNPs on VFA and SFA was additive, and an epistatic effect was not observed.

In summary, we showed that *CYP17A1* rs1004467 and *NT5C2* rs11191548 SNPs are significantly associated with both reduced VFA and SFA in women. Our results suggest that the region encompassing *CYP17A1* to *NT5C2* has a role in reducing visceral and subcutaneous fat mass. However, these results require confirmation in other populations.

CONFLICT OF INTEREST

The authors declare no conflict of interest.

ACKNOWLEDGEMENTS

This work was supported by a Grant-in-Aid from the Ministry of Education, Science, Sports, and Culture of Japan (21591186 to Hotta, K., 23701082 to Kitamoto, T., and 23791027 to Kitamoto, A.), and by the Mitsui Life Science Social Welfare Foundation.

1 Carr, D. B., Utzschneider, K. M., Hull, R. L., Kodama, K., Retzlaff, B. M., Brunzell, J. D. *et al.* Intra-abdominal fat is a major determinant of the National Cholesterol Education Program Adult Treatment Panel III criteria for the metabolic syndrome. *Diabetes* **53,** 2087–2094 (2004).
2 Matsuzawa, Y. Therapy insight: adipocytokines in metabolic syndrome and related cardiovascular disease. *Nat. Clin. Pract. Cardiovasc. Med.* **3,** 35–42 (2006).
3 Hotta, K., Funahashi, T., Bodkin, N. L., Ortmeyer, H. K., Arita, Y., Hansen, B. C. *et al.* Circulating concentrations of the adipocyte protein adiponectin are decreased in parallel with reduced insulin sensitivity during the progression to type 2 diabetes in rhesus monkeys. *Diabetes* **50,** 1126–1133 (2001).
4 Mastuzawa, Y. Metabolic syndrome-definition and diagnostic criteria in Japan. *J. Atheroscler. Thromb.* **12,** 301 (2005).
5 Arai, H., Yamamoto, A., Matsuzawa, Y., Saito, Y., Yamada, N., Oikawa, S. *et al.* Prevalence of metabolic syndrome in the general Japanese population in 2000. *J. Atheroscler. Thromb.* **13,** 202–208 (2006).
6 Selby, J. V., Newman, B., Quesenberry, C. P. Jr., Fabsitz, R. R., Carmelli, D., Meaney, F. J. *et al.* Genetic and behavioral influences on body fat distribution. *Int. J. Obes.* **14,** 593–602 (1990).
7 Rose, K. M., Newman, B., Mayer-Davis, E. J. & Selby, J. V. Genetic and behavioral determinants of waist-hip ratio and waist circumference in women twins. *Obes. Res.* **6,** 383–392 (1998).
8 Souren, N. Y., Paulussen, A. D., Loos, R. J., Gielen, M., Beunen, G., Fagard, R. *et al.* Anthropometry, carbohydrate and lipid metabolism in the East Flanders Prospective Twin Survey: heritabilities. *Diabetologia* **50,** 2107–2116 (2007).
9 Lindgren, C. M., Heid, I. M., Randall, J. C., Lamina, C., Steinthorsdottir, V., Qi, L. *et al.* Genome-wide association scan meta-analysis identifies three loci influencing adiposity and fat distribution. *PLoS Genet.* **5,** e1000508 (2009).
10 Heard-Costa, N. L., Zillikens, M. C., Monda, K. L., Johansson, A., Harris, T. B., Fu, M. *et al.* NRXN3 is a novel locus for waist circumference: a genome-wide association study from the CHARGE Consortium. *PLoS Genet.* **5,** e1000539 (2009).
11 Hotta, K., Nakamura, M., Nakamura, T., Matsuo, T., Nakata, Y., Kamohara, S. *et al.* Polymorphisms in NRXN3, TFAP2B, MSRA, LYPLAL1, FTO and MC4R and their effect on visceral fat area in the Japanese population. *J. Hum. Genet.* **55,** 738–742 (2010).
12 Tanabe, A., Yanagiya, T., Iida, A., Saito, S., Sekine, A., Takahashi, A. *et al.* Functional single-nucleotide polymorphisms in the secretogranin III (SCG3) gene that form secretory granules with appetite-related neuropeptides are associated with obesity. *J. Clin. Endocrinol. Metab.* **92,** 1145–1154 (2007).
13 Yanagiya, T., Tanabe, A., Iida, A., Saito, S., Sekine, A., Takahashi, A. *et al.* Association of single-nucleotide polymorphisms in MTMR9 gene with obesity. *Hum. Mol. Genet.* **16,** 3017–3026 (2007).
14 Thorleifsson, G., Walters, G. B., Gudbjartsson, D. F., Steinthorsdottir, V., Sulem, P., Helgadottir, A. *et al.* Genome-wide association yields new sequence variants at seven loci that associate with measures of obesity. *Nat. Genet.* **41,** 18–24 (2009).
15 Willer, C. J., Speliotes, E. K., Loos, R. J., Li, S., Lindgren, C. M., Heid, I. M. *et al.* Six new loci associated with body mass index highlight a neuronal influence on body weight regulation. *Nat. Genet.* **41,** 25–34 (2009).
16 Meyre, D., Delplanque, J., Chèvre, J. C., Lecoeur, C., Lobbens, S., Gallina, S. *et al.* Genome-wide association study for early-onset and morbid adult obesity identifies three new risk loci in European populations. *Nat. Genet.* **41,** 157–159 (2009).
17 Hotta, K., Kitamoto, T., Kitamoto, A., Mizusawa, S., Matsuo, T., Nakata, Y. *et al.* Computed tomography analysis of the association between SH2B1 rs7498665 single-nucleotide polymorphism and visceral fat area. *J. Hum. Genet.* **56,** 716–719 (2011).
18 Hindorff, L. A., Sethupathy, P., Junkins, H. A., Ramos, E. M., Mehta, J. P., Collins, F. S. *et al.* Potential etiologic and functional implications of genome-wide association loci for human diseases and traits. *Proc. Natl Acad. Sci. USA* **106,** 9362–9367 (2009).
19 Hotta, K., Kitamoto, T., Kitamoto, A., Mizusawa, S., Matsuo, T., Nakata, Y. *et al.* Association of variations in the FTO, SCG3 and MTMR9 genes with metabolic syndrome in a Japanese population. *J. Hum. Genet.* **56,** 647–651 (2011).
20 Levy, D., Ehret, G. B., Rice, K., Verwoert, G. C., Launer, L. J., Dehghan, A. *et al.* Genome-wide association study of blood pressure and hypertension. *Nat. Genet.* **41,** 677–687 (2009).
21 Newton-Cheh, C., Johnson, T., Gateva, V., Tobin, M. D., Bochud, M., Coin, L. *et al.* Genome-wide association study identifies eight loci associated with blood pressure. *Nat. Genet.* **41,** 666–676 (2009).
22 Yoshizumi, T., Nakamura, T., Yamane, M., Islam, A. H., Menju, M., Yamasaki, K. *et al.* Abdominal fat: standardized technique for measurement at CT. *Radiology* **211,** 283–286 (1999).
23 Ohnishi, Y., Tanaka, T., Ozaki, K., Yamada, R., Suzuki, H. & Nakamura, Y. A high-throughput SNP typing system for genome-wide association studies. *J. Hum. Genet.* **46,** 471–477 (2001).
24 Nielsen, D. M., Ehm, M. G. & Weir, B. S. Detecting marker-disease association by testing for Hardy–Weinberg disequilibrium at a marker locus. *Am. J. Hum. Genet.* **63,** 1531–1540 (1998).
25 Wright, S. The genetical structure of populations. *Ann. Eugen.* **15,** 323–354 (1951).
26 Heid, I. M., Jackson, A. U., Randall, J. C., Winkler, T. W., Qi, L., Steinthorsdottir, V. *et al.* Meta-analysis identifies 13 new loci associated with waist-hip ratio and reveals sexual dimorphism in the genetic basis of fat distribution. *Nat. Genet.* **42,** 949–960 (2010).

27 Mitri, J. & Hamdy, O. Diabetes medications and body weight. *Expert Opin. Drug Saf.* **8,** 573–584 (2009).
28 Takeuchi, F., Isono, M., Katsuya, T., Yamamoto, K., Yokota, M., Sugiyama, T. *et al.* Blood pressure and hypertension are associated with 7 loci in the Japanese population. *Circulation* **121,** 2302–2309 (2010).
29 Kilpeläinen, T. O., Zillikens, M. C., Stančákova, A., Finucane, F. M., Ried, J. S., Langenberg, C. *et al.* Genetic variation near IRS1 associates with reduced adiposity and an impaired metabolic profile. *Nat. Genet.* **43,** 753–760 (2011).
30 Gilep, A. A., Sushko, T. A. & Usanov, S. A. At the crossroads of steroid hormone biosynthesis: the role, substrate specificity and evolutionary development of CYP17. *Biochim. Biophys. Acta* **1814,** 200–209 (2011).
31 Itoh, R. IMP–GMP 5′-nucleotidase. *Comp. Biochem. Physiol. B* **105,** 13–19 (1993).
32 Goytain, A. & Quamme, G. A. Functional characterization of ACDP2 (ancient conserved domain protein), a divalent metal transporter. *Physiol. Genomics* **22,** 382–389 (2005).
33 Cordell, H. Detecting gene–gene interactions that underlie human diseases. *Nat. Rev. Genet.* **10,** 392–404 (2009).

Supplementary Information accompanies the paper on Journal of Human Genetics website (http://www.nature.com/jhg)

Epilepsia, 52(5):1010–1017, 2011
doi: 10.1111/j.1528-1167.2011.03046.x

FULL-LENGTH ORIGINAL RESEARCH

Therapy for hyperthermia-induced seizures in *Scn1a* mutant rats

***Keiichiro Hayashi, †Satoshi Ueshima, ‡Mamoru Ouchida, §Tomoji Mashimo, *Teiichi Nishiki, †Toshiaki Sendo, §Tadao Serikawa, *Hideki Matsui, and *Iori Ohmori**

*Department of Physiology, Graduate School of Medicine, Dentistry, and Pharmaceutical Sciences, Okayama University, Okayama, Japan; †Department of Pharmacy, Okayama University Hospital, Okayama, Japan; ‡Department of Molecular Genetics, Graduate School of Medicine, Dentistry, and Pharmaceutical Sciences, Okayama University, Okayama, Japan; and §Institute of Laboratory Animals, Graduate School of Medicine, Kyoto University, Kyoto, Japan

Summary

Purpose: Mutations in the *SCN1A* gene, which encodes the α1 subunit of voltage-gated sodium channels, cause generalized epilepsy with febrile seizures plus (GEFS+) and severe myoclonic epilepsy of infancy (SMEI). N1417H-*Scn1a* mutant rats are considered to be an animal model of human FS+ or GEFS+. To assess the pharmacologic validity of this model, we compared the efficacies of eight different antiepileptic drugs (AEDs) for the treatment of hyperthermia-induced seizures using N1417H-*Scn1a* mutant rats.

Methods: AEDs used in this study included valproate, carbamazepine (CBZ), phenobarbital, gabapentin, acetazolamide, diazepam (DZP), topiramate, and potassium bromide (KBr). The effects of these AEDs were evaluated using the hot water model, which is a model of experimental FS. Five-week-old rats were pretreated with each AED and immersed in water at 45°C to induce hyperthermia-induced seizures. The seizure manifestations and video-electroencephalographic recordings were evaluated. Furthermore, the effects of each AED on motor coordination and balance were assessed using the balance-beam test.

Key Findings: KBr significantly reduced seizure durations, and its anticonvulsant effects were comparable to those of DZP. On the other hand, CBZ decreased the seizure threshold. In addition, DZP and not KBr showed significant impairment in motor coordination and balance.

Significance: DZP and KBr showed potent inhibitory effects against hyperthermia-induced seizures in the *Scn1a* mutant rats, whereas CBZ exhibited adverse effects. These responses to hyperthermia-induced seizures were similar to those in patients with GEFS+ and SMEI. N1417H-*Scn1a* mutant rats may, therefore, be useful for testing the efficacy of new AEDs against FS in GEFS+ and SMEI patients.

KEY WORDS: Febrile seizure, Animal models, *Scn1a* gene, Generalized epilepsy with febrile seizures plus, Severe myoclonic epilepsy of infancy.

Febrile seizures (FS) are the most common convulsive disorder and affect 2–5% of children between the ages of 6 months and 6 years (Verity et al., 1985; Hauser, 1994; Offringa & Moyer, 2001). Although most FS are benign, known as simple FS, and do not require treatment, 2–7% of patients with FS subsequently develop epilepsy (Baulac et al., 2004). Generalized epilepsy with febrile seizures plus (GEFS+) is a familial epileptic syndrome characterized by FS persisting beyond 6 years and subsequent development of various types of epilepsy, including generalized tonic–clonic, myoclonic, and absence seizures (Scheffer & Berkovic, 1997). In severe myoclonic epilepsy of infancy (SMEI; also known as Dravet syndrome), repetitive FS begin in the first year of life, and life-threatening status epilepticus is often provoked by fever. Therefore, appropriate treatment of FS is important for patients with GEFS+ and SMEI.

Heterozygous mutations in *SCN1A*, a gene encoding the α1 subunit in voltage-gated sodium channels ($Na_V1.1$), are responsible for GEFS+ and SMEI. Mutations in *SCN1A* account for 80% of SMEI cases and 10% of GEFS+ cases (Claes et al., 2001; Ohmori et al., 2002; Hattori et al., 2008). Developments in genetic engineering have enabled the generation of various genetically modified animals, and many researchers can now investigate pathology and new disease treatments using these animals.

Recently, Mashimo et al. generated *Scn1a* mutant rats (F344/NSlc-*Scn1a*^{Kyo811}) with the missense mutation,

Accepted February 1, 2011; Early View publication April 11, 2011.
Address correspondence to Iori Ohmori, Department of Physiology, Graduate School of Medicine, Dentistry, and Pharmaceutical Sciences, Okayama University, 5-1 Shikata-cho, 2-chome, Okayama 700-8558, Japan. E-mail: iori@md.okayama-u.ac.jp

N1417H, using ENU mutagenesis (Mashimo et al., 2008, 2010). These N1417H-*Scn1a* mutant rats are considered an animal model of human FS+ or GEFS+. Generally, animal models of human diseases are required to fulfill three criteria, namely face validity, construct validity, and predictive validity (Chadman et al., 2009). Face validity incorporates a conceptual analogy to the symptoms of the human disease. Homozygous N1417H-*Scn1a* mutant rats exhibited susceptibility to hyperthermia-induced seizures, and their seizures persisted over the age of 5 weeks, whereas wild-type rats were unaffected. (Mashimo et al., 2010). Therefore, this model rat showed febrile seizures similar to those seen in patients with GEFS+ and SMEI. Second, construct validity incorporates a conceptual analogy to the cause of the human disease. These rats have an N1417H missense mutation in the causative *SCN1A* gene of GEFS+ and SMEI. N1417H was not detected in human patients, but the electrophysiologic properties of N1417H share a common molecular basis with most of SMEI, and some GEFS+ patients. Namely, the recombinant N1417H-human *SCN1A* mutation was revealed to have a loss-of-function effect on $Na_v1.1$, and the hippocampal neurons of these rats demonstrated impaired biophysical properties of inhibitory γ-aminobutyric acid (GABA)ergic neurons (Mashimo et al., 2010). We have confirmed that N1417H-*Scn1a* mutant rats fulfilled these two criteria in our previous study. Herein, we addressed the third criterion: predictive validity. It incorporates the specificity of responses to treatments that are effective in the human disease. We herein evaluated the efficacy of antiepileptic drugs (AEDs) on hyperthermia-induced seizures in the model rats. Potassium bromide (KBr), a traditionally prescribed AED, was found to be as effective as diazepam (DZP), whereas carbamazepine (CBZ) showed adverse effects. These drug-mediated responses to hyperthermia-induced seizures in the new model rats were similar to those in patients with GEFS+ or SMEI.

Materials and Methods

Animals

Male homozygous N1417H-*Scn1a* mutant rats (F344/NSlc-*Scn1a*^{Kyo811}) (National Bio Resource Project for the Rat in Japan, Kyoto University, Kyoto, Japan) were used to assess the effects of AEDs against hyperthermia-induced seizures. The susceptibility of wild-type rats to hyperthermia decreases with age, and, therefore, these 5-week-old rats showed no indications of hyperthermia-induced seizures, whereas the homozygous N1417H-*Scn1a* mutant rats demonstrated generalized tonic–clonic seizures induced by hyperthermia until at least 10 weeks of age (Mashimo et al., 2010). The rats were maintained under standard laboratory conditions with a 12-h light/dark cycle and food and water ad libitum. All experiments were performed in accordance with protocols approved by the Institutional Animal Care and Use Committee of Okayama University.

Induction of hyperthermia-induced seizures

Experimental FS have been extensively studied in a well-established model in which FS are evoked by exposing the rat pups (postnatal day 8–15) to heated air (Holtzman et al., 1981; Schuchmann et al., 2006), hot water jet on the heads (Ullal et al., 1996), or hot water bathing (Klauenberg & Sparber, 1984). We used hot water bathing from the view point of animal welfare: namely, heated air requires longer exposure of the rats to hyperthermic environment and induces more severe seizures compared with hot water bathing (Fig. S1). Induction of hyperthermia-induced seizures was performed as described previously, with slight modifications (Mashimo et al., 2010). Hyperthermia was induced by placing the rats in a 19.0 × 24.7 × 15.5 cm water bath (Thermo minder SD mini, Taitec, Japan) filled with water at 45°C to a depth of 6 cm (Fig. 1A). The rats were kept in the water for a maximum of 5 min or until a seizure occurred. We confirmed that immersing the rats in 37 and 40°C water for 5 min did not evoke seizures (Fig. S2). When a seizure occurred, the rats were removed immediately from the bath and monitored until they recovered. Rectal temperature of the rats was measured immediately after seizure onset using a digital thermometer (BDT-100; Bioresearch Center, Aichi, Japan) connected to a rectal probe (Ret-2; Physitemp, Clifton, NJ, U.S.A.). Each rat was assigned a score based on the most severe seizure observed. The seizure parameters were scored as follows: (0) no response; (1) head nodding with brief twitching movements (Fig. 1B); (2) repetitive myoclonic jerks with postural tone (Fig. 1C); (3) jumping and/or running fits (Fig. 1D); (4) generalized tonic–clonic seizure with loss of postural tone (Fig. 1E); and (5) death due to continuous convulsions. Seizure parameters were scored by an investigator who was blinded to the treatment received. All procedures were recorded using a video camera.

Treatment with AEDs

To assess the pharmacologic validation of N1417H-*Scn1a* mutant rats, AEDs that have been established to be effective in patients with GEFS+ and SMEI were chosen. AEDs used in the present study included sodium valproate (VPA-Na; Sigma-Aldrich, Tokyo, Japan), phenobarbital sodium (PB-Na; Wako, Osaka, Japan), diazepam (DZP; Wako), carbamazepine (CBZ; Sigma-Aldrich), acetazolamide sodium (AZA-Na, Diamox; Sanwa, Aichi, Japan), potassium bromide (KBr; Wako), topiramate (TPM; Toronto Research Chemicals, Toronto, ON, Canada), and gabapentin (GBP; Toronto Research Chemicals). VPA-Na, PB-Na, AZA-Na, KBr, and GBP were dissolved in saline. CBZ, DZP, and TPM were suspended in 10% polyethylene glycol 400 with saline. The rats were fasted overnight and orally administered each AED. Experimental conditions were determined based on the results of preliminary studies (Fig. S3). Because the appropriate range of each AED for the model rats is not known, we referred to the doses used to treat human epilepsy. The therapeutic range of each AED was

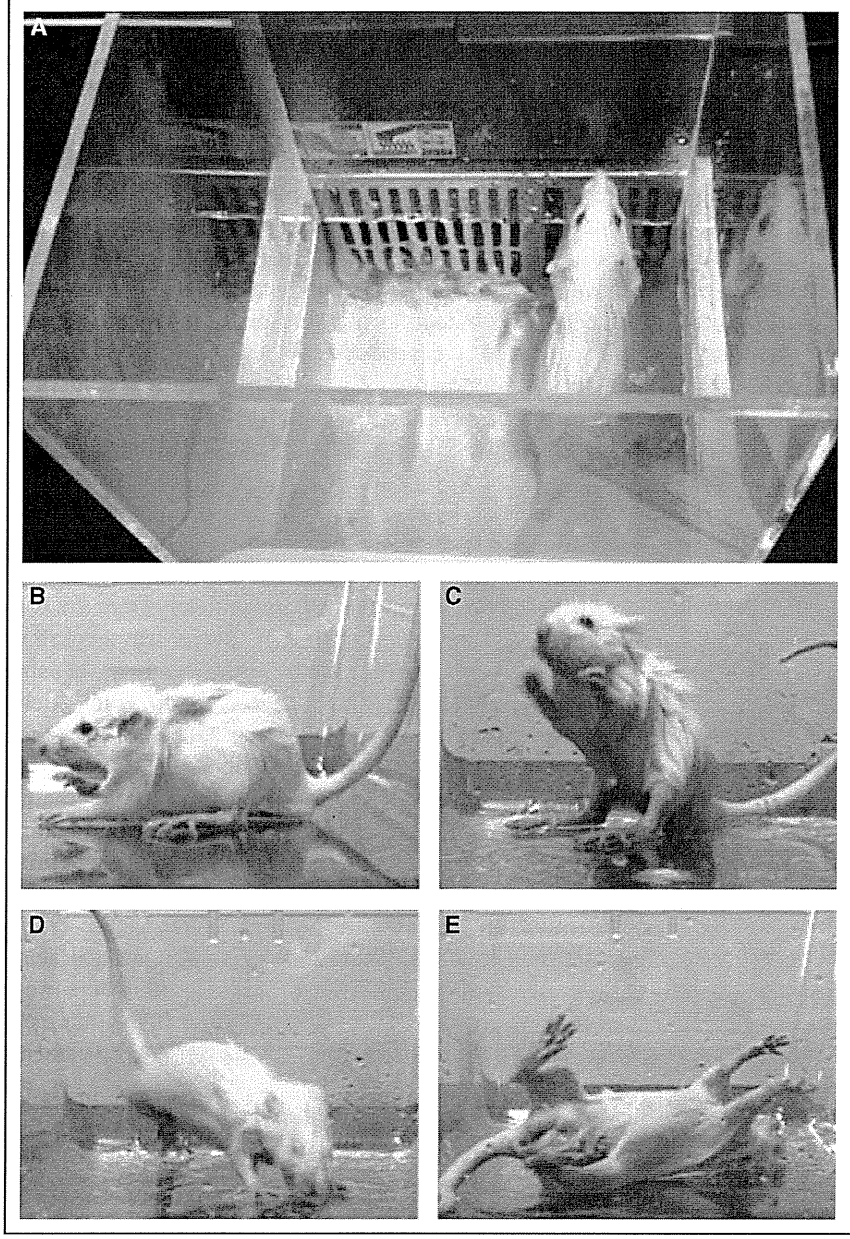

Figure 1.
Hyperthermia-induced seizures in *Scn1a* mutant rats. (**A**) Hyperthermia was induced by placing the rats in a water bath filled with water at 45°C. (**B**) Head nodding and brief twitching movements were classified as a score of 1. (**C**) Repetitive myoclonic jerks of the forelimbs with a postural tone were classified as a score of 2. (**D**) Jumping and/or running fits were classified as a score of 3. (**E**) Generalized tonic–clonic seizures with loss of postural tone were classified as a score of 4. *Epilepsia* © ILAE

determined according to previous literature as follows; VPA, 40–120 μg/ml (Schmidt, 2009); CBZ, 4–12 μg/ml (Eadie, 2001); PB, 10–40 μg/ml (Schmidt, 2009); GBP, 2–20 μg/ml (McLean, 1999); AZA, 10–20 μg/ml (Granero et al., 2007); DZP, 0.2–0.6 μg/ml (Ogutu et al., 2002); and KBr, 500–1,500 μg/ml (Ryan & Baumann, 1999). In cases where the blood concentration did not reach the therapeutic range, a higher dose was administrated to achieve a concentration higher than the top of the therapeutic range of each AED. Seizures were induced when the blood concentration of each AED elevated to an adequate level. VPA-Na (200 mg/kg) was administered for 30 min; CBZ (200 mg/kg), 120 min; PB-Na (50 mg/kg), 240 min; GBP (100 mg/kg), 90 min; AZA-Na (55 mg/kg), 30 min; DZP (5 mg/kg), 15 min; TPM (80 mg/kg), 90 min; and KBr (1,800 mg/kg), 90 min before seizures were induced. Experimental conditions of DZP and TPM administration were determined based on previous studies (Ishihara et al., 2000; Borowicz et al., 2003; Sendrowski et al., 2007). The temperature threshold was measured using the rectal temperature of the rats immediately after seizure onset, in addition to the duration of the seizure and the seizure severity score. After seizure termination, blood samples were obtained from the tail vein of the rats, and the blood concentration of each AED was then measured. Measurement of the blood concentrations of each AED was performed as described in Data S1.

Electroencephalography

Ictal electroencephalography (EEG) patterns were also analyzed for four AEDs (AZA, TPM, DZP, and KBr), which

exhibit remarkable therapeutic effects and CBZ, which may aggravate hyperthermia-induced seizures. At 4 weeks of age, the rats were implanted with electrodes for EEG recordings. Under pentobarbital sodium anesthesia (35 mg/kg, i.p., Nembutal; Abbott Laboratories, Abbott Park, IL, U.S.A.), the rats were fixed to a stereotaxic apparatus (SR-5M; Narishige, Tokyo, Japan). Stainless steel screw electrodes (2.0 Ø × 0.6 × 1.7 mm; Fukuoka Seimitsu, Fukuoka, Japan) were implanted bilaterally into the frontal cortex (AP: +0.5 mm; ML: ±3.0 mm from bregma) and occipital cortex (AP: −7.0 mm; ML: ±3.0 mm from bregma). In addition, a stainless steel screw implanted into the posterior end of the skull served as a reference electrode. This assembly was fixed to the skull with dental cement (UNIFAST II; GC Dental Products, Aichi, Japan). After a 1-week recovery period, cortical EEG was recorded (Neurofax EEG-1200; Nihon Koden, Tokyo, Japan). The duration of the seizure discharges between seizure onset and termination were analyzed.

Balance-beam test

Each AED has various side effects on the central nervous system, gastrointestinal organs, urinary tracts, and so on, especially following chronic use. In the present study, we assessed only the acute effects on motor coordination and balance because AEDs were administered as a single dose. This test was performed as described previously, with slight modifications (Carter et al., 1999; Perez & Palmiter, 2005). The beam was 105 cm long and 35 mm wide, and it was elevated 100 cm above the ground. A black box (20 × 18 × 30 cm) was set at one end of the beam as the goal. A bright light was situated opposite the goal box to encourage the rats to cross the beam (Fig. 5A). The rats were first trained to traverse the beam and were then tested. Crossing time and the number of footfalls were recorded.

Statistical analysis

Data are presented as mean ± standard error of the mean (SEM). Data analyses were performed using nonrepeated measures analysis of variance (ANOVA) with Dunnett's post hoc test. Seizure severity scores were analyzed using the Kruskal-Wallis *H* test together with the Mann-Whitney *U*-test, followed by the Bonferroni correction post hoc test. Statistical difference was defined as $p < 0.05$.

Results

Effects of AEDs on hyperthermia-induced seizures

In order to evaluate which AEDs are effective against hyperthermia-induced seizures in *Scn1a* mutant rats, we induced seizures by immersing the rats pretreated with each AED in water at 45°C. The anticonvulsant effects of AEDs were assessed using four parameters: incidence of seizure; temperature threshold, calculated from the rectal temperature of the rats immediately after seizure onset; seizure duration; and seizure severity score. DZP and KBr, but no other AEDs, reduced the incidence rate of hyperthermia-induced seizures (Fig. 2A). PB, DZP, TPM, and KBr significantly increased the temperature threshold, whereas CBZ, GBP, and AZA decreased the threshold (Fig. 2B). All AEDs, except CBZ, significantly decreased the seizure duration (Fig. 2C). In particular, AZA, DZP, and KBr shortened the seizure duration dramatically (Fig. 2C). Although DZP and KBr tended to reduce the seizure severity scores, significant changes were not observed (Fig. 2D).

After seizure termination, blood samples were obtained from the tail vein of the rats, and blood concentrations of the AEDs were then measured. Blood concentrations of all AEDs, except those of DZP, increased over the therapeutic range (Table 1). Although the serum level of

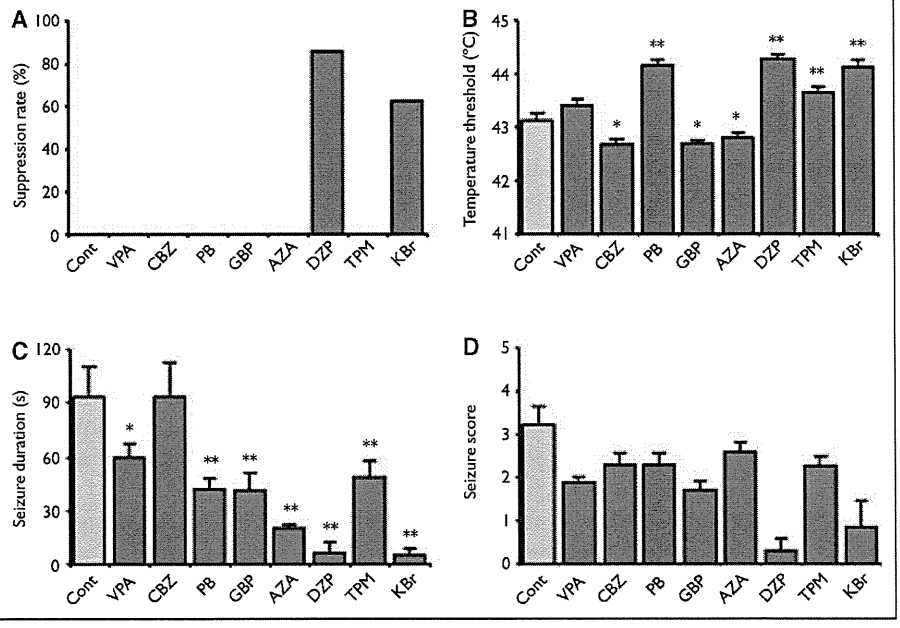

Figure 2.
Comparison of effects of AEDs on hyperthermia-induced seizures in *Scn1a* mutant rats. (**A**) Suppression rate of seizures (%). (**B**) Temperature threshold. Rectal temperature of the rats was measured immediately after seizure onset. (**C**) Seizure duration. (**D**) Seizure severity score. Untreated (Cont., n = 9), VPA-Na (200 mg/kg, n = 8), CBZ (200 mg/kg, n = 7), PB-Na (50 mg/kg, n = 7), GBP (100 mg/kg, n = 7), AZA-Na (55 mg/kg, n = 12), DZP (5 mg/kg, n = 7), TPM (80 mg/kg, n = 8), and KBr (1,800 mg/kg, n = 7). Data are mean ± SEM. *p < 0.05, **p < 0.01 compared to controls (untreated).

Table 1. Blood concentrations of antiepileptic drugs immediately after hyperthermia-induced seizures in *Scn1a* mutant rats

	n	Dose (mg/kg)	Blood level (μg/ml)	Therapeutic range (μg/ml)	References
VPA	8	200	174.7 ± 22.8	40–120	Schmidt, 2009
CBZ	7	200	13.2 ± 1.7	4–12	Eadie, 2001
PB-Na	7	50	40.3 ± 0.8	12–30	Schmidt, 2009
GBP	7	100	33.5 ± 1.4	2–20	McLean, 1999
AZA-Na	12	55	49.8 ± 4.0	10–20	Granero et al., 2007
DZP	7	5	0.15 ± 0.04	0.2–0.6	Ogutu et al., 2002
TPM	8	80	n.d.	–	–
KBr	7	1800	1769.1 ± 204.7	500–1500	Ryan & Baumann, 1999

Data are mean ± SEM.

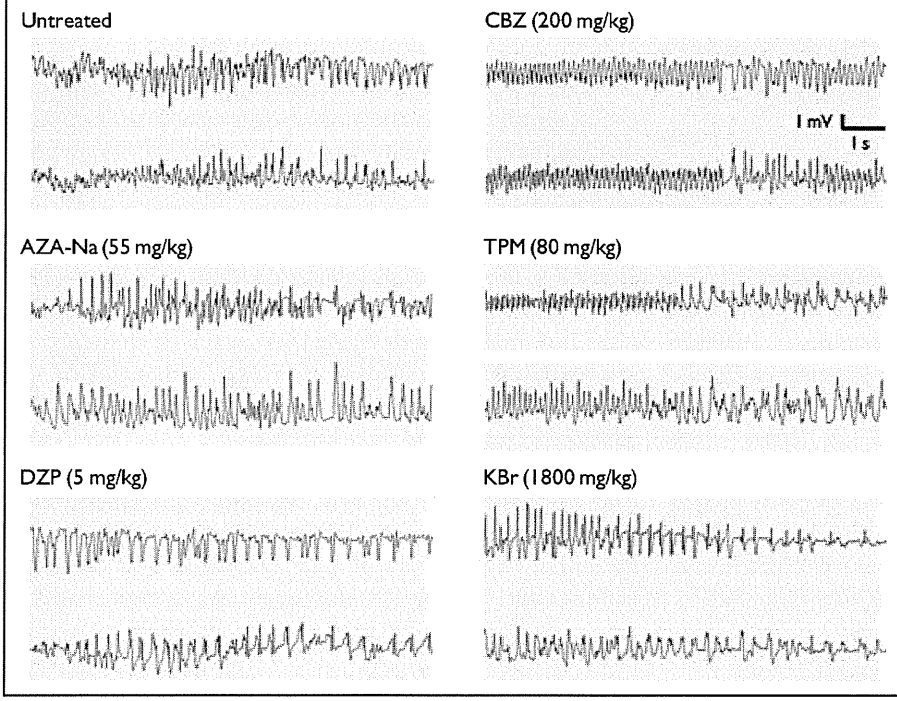

Figure 3.
Representative ictal EEG patterns of a hyperthermia-induced seizure after treatment with each AED. The top and bottom traces were from the frontal and occipital cortices, respectively.
Epilepsia © ILAE

DZP did not reach the therapeutic range in the 5 mg/kg DZP-treated group, these rats showed ataxia and lethargy in the hot bath; therefore, the dose of DZP was not increased. We could not exclude the possibility that higher doses of some of AEDs may have lead to the different results.

Electroencephalography

Ictal EEG patterns were examined in five AEDs (AZA, TPM, DZP, KBr, and CBZ). Representative ictal EEG recordings from the rats are shown in Figs 3 and 4A. It was observed that seizures began as tonic seizures with high frequency spikes, followed by clonic seizures (Fig. 4A). Hyperthermia-induced seizures in *Scn1a* mutant rats were often provoked as several recurrent seizures with a few seconds interval between the seizures. Before the second tonic–clonic seizure occurs, interictal spikes appear and gradually increase their amplitude. Between the first seizure and the second seizure, high amplitude spikes were associated with myoclonic jerks. We analyzed the duration of the seizure discharges on EEGs between seizure onset and termination (Fig. 4A). AZA, DZP, and KBr significantly reduced the duration of the seizure discharges, whereas CBZ and TPM showed no significant changes (Fig. 4B).

Balance-beam test

Motor coordination and balance were examined using the balance-beam test for some of the AEDs which showed remarkable inhibitory effects on hyperthermia-induced seizures (Fig. 5A,B). Although control (i.e., untreated) rats walked along the beam with ease, motor deficits were observed in the PB- and DZP-treated groups (Fig. 5C,D). On the other hand, AZA and KBr did not affect motor coordination or balance (Fig. 5C,D).

Discussion

In total, >600 mutations in the *SCN1A* gene have been identified in patients with SMEI and GEFS+. *SCN1A* is the most representative mutated gene in human fever-related epileptic syndromes. Patients with SMEI have life-threatening status epilepticus, which is often provoked by fever, and patients with GEFS+ have repetitive FS that can persist beyond 6 years. Therefore, induction of appropriate treatments for FS in the early stages of onset is essential for these patients.

Rodent models harboring the responsible mutant genes are often used to elucidate the molecular pathogenesis and to cultivate novel treatments. *Scn1a* KO mice (Yu et al., 2006; Ogiwara et al., 2007) and R1648H-*Scn1a* mice (Martin et al., 2010) were generated to investigate the *SCN1A* gene. Both types of heterozygous mutant mice exhibited susceptibility to hyperthermia-induced seizures (Oakley et al., 2009; Martin et al., 2010). Homozygous N1417H-*Scn1a* mutant rats in the present study also exhibited susceptibility to hyperthermia-induced seizures.

In the present study, the effects of AEDs on hyperthermia-induced seizures were assessed in homozygous N1417H-*Scn1a* mutant rats. DZP and KBr showed potent effects on hyperthermia-induced seizures in these rats. DZP and KBr demonstrated reduction in the incidence of seizures, increase in the temperature threshold, and shortening of the seizure duration. Furthermore, DZP and KBr also decreased the duration of the seizure discharges on EEG. In the balance-beam test, DZP significantly increased the crossing time and total number of footfalls, whereas KBr did not demonstrate a significant effect on these parameters. Together with the blood level of each AED, these results suggested that DZP in low doses, but not KBr in high doses, influences motor coordination and balance. When the pharmacokinetics between DZP and KBr were compared, DZP was shown to be effective in the short term, whereas KBr was shown to have a long half-life (12 days) in blood. Development of tolerance to DZP in long-term treatment is well known (Haigh & Feely, 1988). Given that DZP is the first choice for treatment of status epilepticus because of its potent anticonvulsant effects, prolonged administration of DZP may decrease the effectiveness of stopping seizures in case of status epilepticus. Therefore, KBr may be recommended for repetitive FS.

PB, VPA, and TPM also showed efficacy for preventing hyperthermia-induced seizures. AZA and GBP decreased the seizure threshold but shortened the duration of seizures. However, the molecular mechanisms that induce hyperthermia-induced seizures and terminate seizures remain unknown. The results presented herein suggest that the mechanisms that increase the seizure threshold and terminate seizures are different. Although AZA is used mainly for treating absence seizures, its ability to shorten seizures is remarkable. Hyperthermia-induced respiratory alkalosis involves the onset of hyperthermia-induced seizures (Schuchmann et al., 2006), and metabolic acidosis terminates seizures and prevents seizure progression (Ziemann et al., 2008). AZA, a carbonic anhydrase inhibitor, is known to cause metabolic acidosis. In fact, AZA-Na (55 mg/kg) decreased the peripheral venous blood pH of rats from 7.38 ± 0.01 to 7.22 ± 0.01 within 30 min of oral administration. This acidosis may have been partially responsible

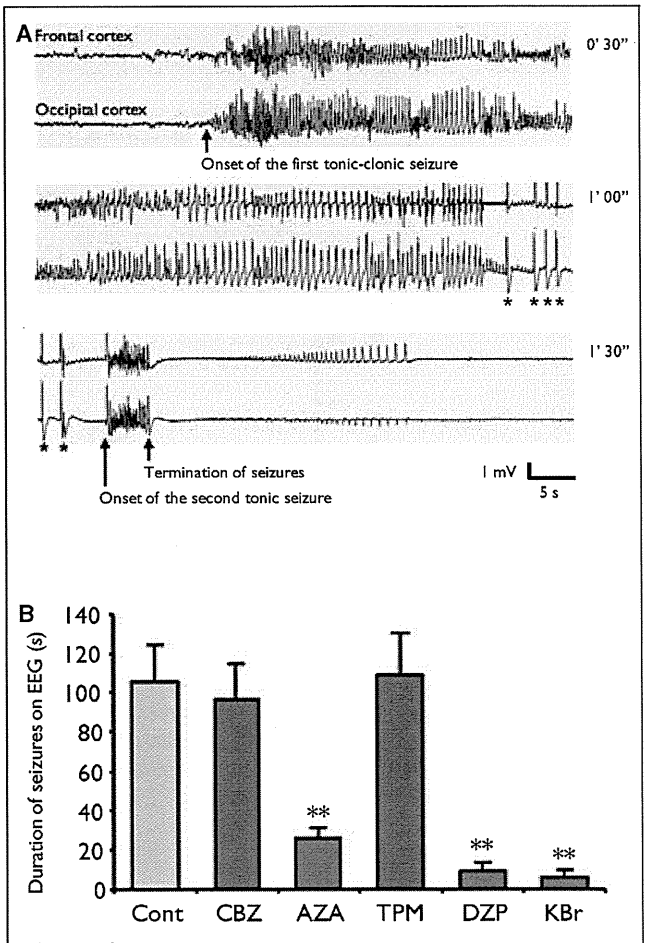

Figure 4.
A representative ictal EEG of a hyperthermia-induced seizure from *Scn1a* mutant rats. (**A**) A seizure began as tonic seizures (the first arrow) with high frequency spikes, followed by clonic seizures. Hyperthermia-induced seizures were often provoked as several recurrent seizures with a few-second interval between the seizures. Before the second tonic seizure occurs (the second arrow), high amplitude spikes were associated with myoclonic jerks. The asterisk (*) indicates myoclonic jerks. After the termination of seizures, repetitive spikes continued for several seconds with no seizure manifestations. (**B**) The duration of the seizure discharges between seizure onset (the first arrow) and termination (the third arrow) was measured. Untreated (Cont., n = 8), CBZ (200 mg/kg, n = 6), AZA-Na (55 mg/kg, n = 7), TPM (80 mg/kg, n = 6), DZP (5 mg/kg, n = 8), and KBr (1,800 mg/kg, n = 7). Data are mean ± SEM. *p < 0.05, **p < 0.01 compared to controls (untreated).
Epilepsia © ILAE

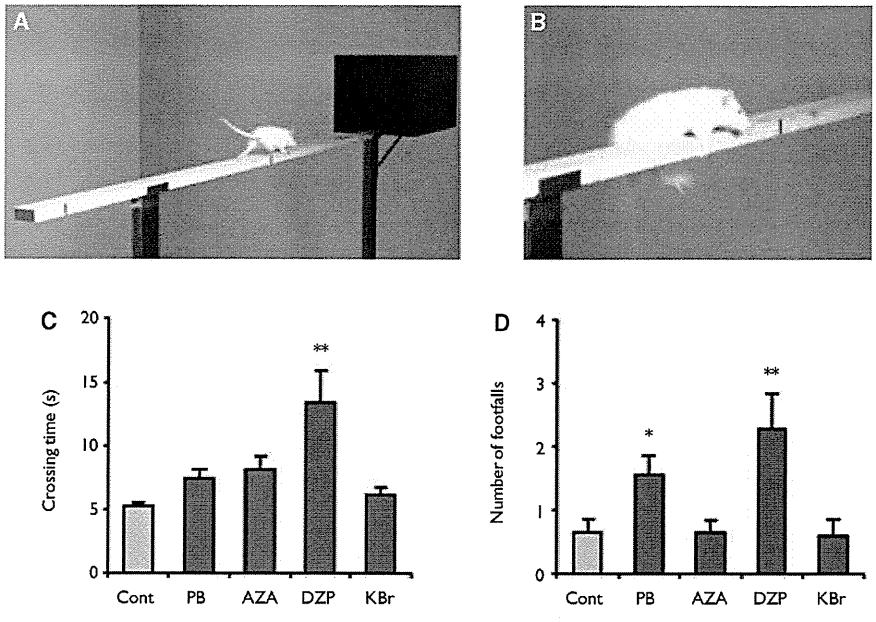

Figure 5.
Balance-beam test apparatus for measuring motor coordination and balance. (**A**) A bright light was placed opposite the black box to encourage the rats to perform the task. The time they took to cross the beam was recorded. (**B**) The number of times the hind limb slipped off the beam was counted. (**C**) Time to cross the beam after treatment with each AED. (**D**) Number of footfalls while crossing the beam after treatment with each AED. Untreated (Cont., n = 14), PB-Na (50 mg/kg, n = 15), AZA-Na (55 mg/kg, n = 14), DZP (5 mg/kg, n = 7), and KBr (1,800 mg/kg, n = 10). Data are mean ± SEM. *p < 0.05, **p < 0.01 compared to controls (untreated).

for decrease in the seizure duration in the AZA-treated group. These findings suggest that AZA is useful for terminating prolonged seizures, but not for inhibiting seizure onset.

Almost all AEDs have a partial effect on hyperthermia-induced seizures. CBZ, on the other hand, significantly reduced the seizure threshold, suggesting that CBZ may aggravate hyperthermia-induced seizures because of its sodium channel blocking effects (Macdonald, 2002).

Taken together, KBr and DZP are first-line treatments for hyperthermia-induced seizures in *Scn1a* mutant rats; PB, TPM, and VPA are second-line treatments. It was observed that AZA suppressed and CBZ aggravated hyperthermia-induced seizures. However, how much of these results in the *Scn1a* mutant rats mimic the results of human epilepsy with *SCN1A* mutation? In patients with SMEI, of which >80% have a mutation in *SCN1A*, benzodiazepines and VPA are effective in preventing seizures (Ceulemans et al., 2004). KBr also improved generalized tonic–clonic seizures, generalized clonic seizures, and complex partial seizures (Oguni et al., 1994). KBr is known to induce several adverse effects such as drowsiness, headache, acneiform rashes, and loss of appetite. The significant toxicity associated with their use and the availability of safer AEDs may lead to a decrease in the use of KBr. The inhibitory effects of TPM as monotherapy were almost equal to those induced by VPA and PB. The clinical efficacy of TPM as adjunctive therapy has been reported in patients with SMEI (Nieto-Barrera et al., 2000, Coppola et al., 2002). Regarding the adverse effects of CBZ in the model rats, CBZ also aggravated seizures in patients with SMEI and GEFS+ (Horn et al., 1986; Guerrini et al., 1998). These reports in humans are consistent with the results presented here in the *Scn1a* mutant rats. *Scn1a* mutant rats seem to reflect considerably the pathogenesis of human *SCN1A* mutation–associated epilepsy. Considering the many differences, such as the way of treatment, treatment dose, type of seizure, age, gender, genetic background, and environmental factors, these rats may be useful for screening new AEDs or novel treatments for FS associated with *SCN1A* mutations in order to predict drugs that might be effective in human patients.

Acknowledgments

We are thankful to Prof. Chiaki Kamei for technical support regarding the EEG recordings. We are thankful to the National Bio Resource Project for the Rat in Japan (http://www.anim.med.kyoto-u.ac.jp/NBR/) for providing rat strains (F344/NSlc-*Scn1a*^{Kyo811}). This work was supported by a Grant-in-Aid from the Ministry of Education, Culture, Sports, Science, and Technology (No. 21390312 to I.O.).

Disclosure

We confirm that we have read the Journal's position on issues involved in ethical publication and affirm that this report is consistent with those guidelines. None of the authors has any conflict of interest to disclose.

References

Baulac S, Gourfinkel-An I, Nabbout R, Huberfeld G, Serratosa J, Leguern E, Baulac M. (2004) Fever, genes, and epilepsy. *Lancet Neurol* 3:421–430.

Borowicz KK, Luszczki JJ, Duda AM, Czuczwar SJ. (2003) Effect of topiramate on the anticonvulsant activity of conventional antiepileptic drugs in two models of experimental epilepsy. *Epilepsia* 44: 640–646.

Carter RJ, Lione LA, Humby T, Mangiarini L, Mahal A, Bates GP, Dunnett SB, Morton AJ. (1999) Characterization of progressive motor deficits in mice transgenic for the human Huntington's disease mutation. *J Neurosci* 19:3248–3257.

Ceulemans B, Boel M, Claes L, Dom L, Willekens H, Thiry P, Lagae L. (2004) Severe myoclonic epilepsy in infancy: toward an optimal treatment. *J Child Neurol* 19:516–521.

Chadman KK, Yang M, Crawley JN. (2009) Criteria for validating mouse models of psychiatric diseases. *Am J Med Genet B Neuropsychiatr Genet* 150B:1–11.

Claes L, Del-Favero J, Ceulemans B, Lagae L, Van Broeckhoven C, De Jonghe P. (2001) De novo mutations in the sodium-channel gene SCN1A cause severe myoclonic epilepsy of infancy. *Am J Hum Genet* 68:1327–1332.

Coppola G, Capovilla G, Montagnini A, Romeo A, Spanò M, Tortorella G, Veggiotti P, Viri M, Pascotto A. (2002) Topiramate as add-on drug in severe myoclonic epilepsy in infancy: an Italian multicenter open trial. *Epilepsy Res* 49:45–48.

Eadie MJ. (2001) Therapeutic drug monitoring – antiepileptic drugs. *Br J Clin Pharmacol* 52(suppl 1):11S–20S.

Granero GE, Longhi MR, Becker C, Junginger HE, Kopp S, Midha KK, Shah VP, Stavchansky S, Dressman JB, Barends DM. (2007) Biowaiver monographs for immediate release solid oral dosage forms: Acetazolamide. *J Pharm Sci* 97:3691–3699.

Guerrini R, Dravet C, Genton P, Belmonte A, Kaminska A, Dulac O. (1998) Lamotrigine and seizure aggravation in severe myoclonic epilepsy. *Epilepsia* 39:508–512.

Haigh JR, Feely M. (1988) Tolerance to the anticonvulsant effect of benzodiazepines. *Trends Pharmacol Sci* 9:361–366.

Hattori J, Ouchida M, Ono J, Miyake S, Maniwa S, Mimaki N, Ohtsuka Y, Ohmori I. (2008) A screening test for the prediction of Dravet syndrome before one year of age. *Epilepsia* 49:626–633.

Hauser WA. (1994) The prevalence and incidence of convulsive disorders in children. *Epilepsia* 35(suppl 2):S1–S6.

Holtzman D, Obana K, Olson J. (1981) Hyperthermia-induced seizures in the rat pup: a model for febrile convulsions in children. *Science* 213:1034–1036.

Horn CS, Ater SB, Hurst DL. (1986) Carbamazepine-exacerbated epilepsy in children and adolescents. *Pediatr Neurol* 2:340–345.

Ishihara K, Kushida H, Yuzurihara M, Wakui Y, Yanagisawa T, Kamei H, Ohmori S, Kitada M. (2000) Interaction of drugs and Chinese herbs: pharmacokinetic changes of tolbutamide and diazepam caused by extract of Angelica dahurica. *J Pharm Pharmacol* 52:1023–1029.

Klauenberg BJ, Sparber SB. (1984) A kindling-like effect induced by repeated exposure to heated water in rats. *Epilepsia* 25:292–301.

Macdonald RL. (2002) Carbamazepine. In Levy RH, Mattson RH, Meldrum BS, Perucca E (Eds) *Antiepileptic drugs*. Lippincott Williams & Wilkins, Philadelphia, pp. 227–235.

Martin MS, Dutt K, Papale LA, Dubé CM, Dutton SB, de Haan G, Shankar A, Tufik S, Meisler MH, Baram TZ, Goldin AL, Escayg A. (2010) Altered function of the SCN1A voltage-gated sodium channel leads to gamma-aminobutyric acid-ergic (GABAergic) interneuron abnormalities. *J Biol Chem* 285:9823–9834.

Mashimo T, Yanagihara K, Tokuda S, Voigt B, Takizawa A, Nakajima R, Kato M, Hirabayashi M, Kuramoto T, Serikawa T. (2008) An ENU-induced mutant archive for gene targeting in rats. *Nat Genet* 40:514–515.

Mashimo T, Ohmori I, Ouchida M, Ohno Y, Tsurumi T, Miki T, Wakamori M, Ishihara S, Yoshida T, Takizawa A, Kato M, Hirabayashi M, Sasa M, Mori Y, Serikawa T. (2010) A missense mutation of the gene encoding voltage-dependent sodium channel (Nav1.1) confers susceptibility to febrile seizures in rats. *J Neurosci* 30:5744–5753.

McLean M. (1999) Gabapentin in the management of convulsive disorders. *Epilepsia* 40(suppl 6):S39–S50; discussion S73–S74.

Nieto-Barrera M, Candau R, Nieto-Jimenez M, Correa A, del Portal LR. (2000) Topiramate in the treatment of severe myoclonic epilepsy in infancy. *Seizure* 9:590–594.

Oakley JC, Kalume F, Yu FH, Scheuer T, Catterall WA. (2009) Temperature- and age-dependent seizures in a mouse model of severe myoclonic epilepsy in infancy. *Proc Natl Acad Sci U S A* 106:3994–3999.

Offringa M, Moyer VA. (2001) Evidence based paediatrics: evidence based management of seizures associated with fever. *BMJ* 323:1111–1114.

Ogiwara I, Miyamoto H, Morita N, Atapour N, Mazaki E, Inoue I, Takeuchi T, Itohara S, Yanagawa Y, Obata K, Furuichi T, Hensch TK, Yamakawa K. (2007) Na(v)1.1 localizes to axons of parvalbumin-positive inhibitory interneurons: a circuit basis for epileptic seizures in mice carrying an Scn1a gene mutation. *J Neurosci* 27:5903–5914.

Oguni H, Hayashi K, Oguni M, Mukahira A, Uehara T, Fukuyama Y, Umezu R, Izumi T, Hara M. (1994) Treatment of severe myoclonic epilepsy in infants with bromide and its borderline variant. *Epilepsia* 35:1140–1145.

Ogutu BR, Newton CR, Crawley J, Muchohi SN, Otieno GO, Edwards G et al. (2002) Pharmacokinetics and anticonvulsant effects of diazepam in children with severe falciparum malaria and convulsions. *Br J Clin Pharmacol* 53:49–57.

Ohmori I, Ouchida M, Ohtsuka Y, Oka E, Shimizu K. (2002) Significant correlation of the SCN1A mutations and severe myoclonic epilepsy in infancy. *Biochem Biophys Res Commun* 295:17–23.

Perez FA, Palmiter RD. (2005) Parkin-deficient mice are not a robust model of parkinsonism. *Proc Natl Acad Sci U S A* 102:2174–2179.

Ryan M, Baumann RJ. (1999) Use and monitoring of bromides in epilepsy treatment. *Pediatr Neurol* 21:523–528.

Scheffer IE, Berkovic SF. (1997) Generalized epilepsy with febrile seizures plus. A genetic disorder with heterogeneous clinical phenotypes. *Brain* 120:479–490.

Schmidt D. (2009) Drug treatment of epilepsy: options and limitations. *Epilepsy Behav* 15:56–65.

Schuchmann S, Schmitz D, Rivera C, Vanhatalo S, Salmen B, Mackie K, Sipilä ST, Voipio J, Kaila K. (2006) Experimental febrile seizures are precipitated by a hyperthermia-induced respiratory alkalosis. *Nat Med* 12:817–823.

Sendrowski K, Sobaniec W, Sobaniec-Lotowska ME, Artemowicz B. (2007) Topiramate as a neuroprotectant in the experimental model of febrile seizures. *Adv Med Sci* 52(suppl 1):161–165.

Ullal GR, Satishchandra P, Shankar SK. (1996) Hyperthermic seizures: an animal model for hot-water epilepsy. *Seizure* 5:221–228.

Verity CM, Butler NR, Golding J. (1985) Febrile convulsions in a national cohort followed up from birth. I – Prevalence and recurrence in the first five years of life. *Br Med J (Clin Res Ed)* 290:1307–1310.

Yu FH, Mantegazza M, Westenbroek RE, Robbins CA, Kalume F, Burton KA, Spain WJ, McKnight GS, Scheuer T, Catterall WA. (2006) Reduced sodium current in GABAergic interneurons in a mouse model of severe myoclonic epilepsy in infancy. *Nat Neurosci* 9:1142–1149.

Ziemann AE, Schnizler MK, Albert GW, Severson MA, Howard MA III, Welsh MJ, Wemmie JA. (2008) Seizure termination by acidosis depends on ASIC1a. *Nat Neurosci* 11:816–822.

Supporting Information

Additional Supporting Information may be found in the online version of this article:

Data S1. Methods.

Figure S1. Comparison of the methods for the induction of hyperthermia-induced seizures in *Scn1a* mutant rats.

Figure S2. Susceptibility of *Scn1a*-N1417H missense mutant rats to water bathing stimuli.

Figure S3. Concentration–time profiles of AEDs after oral administration in 8- to 10-week-old male rats.

Please note: Wiley-Blackwell is not responsible for the content or functionality of any supporting information supplied by the authors. Any queries (other than missing material) should be directed to the corresponding author for the article.

Published in final edited form as:
Nature. ; 478(7367): 114–118. doi:10.1038/nature10490.

Endonuclease G is a novel determinant of cardiac hypertrophy and mitochondrial function

Chris McDermott-Roe[1], **Junmei Ye**[2], **Rizwan Ahmed**[1], **Xi-Ming Sun**[1], **Anna Serafín**[3], **James Ware**[1], **Leonardo Bottolo**[1], **Phil Muckett**[1], **Xavier Cañas**[3], **Jisheng Zhang**[2], **Glenn C. Rowe**[4], **Rachel Buchan**[1], **Han Lu**[1], **Adam Braithwaite**[1], **Massimiliano Mancini**[5], **David Hauton**[6], **Ramon Martí**[7], **Elena García-Arumí**[7], **Norbert Hubner**[8,9], **Howard Jacob**[10], **Tadao Serikawa**[11], **Vaclav Zidek**[12], **Frantisek Papousek**[12], **Frantisek Kolar**[12], **Maria Cardona**[2], **Marisol Ruiz-Meana**[13], **David García-Dorado**[13], **Joan X Comella**[14], **Leanne E Felkin**[15], **Paul JR Barton**[15,16], **Zoltan Arany**[4], **Michal Pravenec**[12], **Enrico Petretto**[1,17], **Daniel Sanchis**[2], and **Stuart A. Cook**[1,16]

[1]Medical Research Council Clinical Sciences Centre, Faculty of Medicine, Imperial College London, Hammersmith Hospital, Du Cane Road, London W12 ONN, UK

[2]Cell Signaling & Apoptosis Group, University Lleida, Biomedical Research Institute of Lleida (IRBLLEIDA), Av Rovira Roure, 80, 25198 Lleida, Spain

[3]Platform of Applied Research on Laboratory Animal Barcelona Science Park, Baldiri Reixac, 4, 08028 Barcelona, Spain

[4]Cardiovascular Institute, Beth Israel Deaconess Medical Institute, CLS906, 3 Blackfan Circle, Boston MA 02215, USA

[5]Department of Radiological, Oncological and Anatomo-Pathological Sciences, Sapienza, University of Rome, Italy

[6]School of Clinical and Experimental Medicine, College of Medical and Dental Sciences, University of Birmingham, Edgbaston, Birmingham, B15 2TT

[7]Unitat de Patologia Mitocondrial i Neuromuscular, Institut de Recerca Hospital Universitari Vall d'Hebron, Universitat Autònoma de Barcelona, Barcelona, Spain

[8]Max-Delbrück Center for Molecular Medicine, Robert-Rössle-Strasse 10, 13125 Berlin, Germany

[9]CC4, Campus Charité Mitte, Charité - Universitätsmedizin Berlin, Charitéplatz 1, 10117 Berlin, Germany

[10]Department of Physiology, Medical College of Wisconsin, Milwaukee WI 53226, U.S.A.

[11]Institute of Laboratory Animals, Graduate School of Medicine, Kyoto University, Yoshidakonoe-cho, Sakyo-ku, Kyoto 606-8501, Japan

[12]Institute of Physiology, Academy of Sciences of the Czech Republic, Vídenska 1083, 142 20 Prague 4, Czech Republic

[13]Grup de Patologia Cardiovascular, Institut de Recerca Hospital Universitari Vall d'Hebron, Universitat Autònoma de Barcelona, Barcelona, Spain

Correspondence and requests: stuart.cook@imperial.ac.uk or daniel.sanchis@cmb.udl.cat .

Author contributions C.M-R, J.Y., X-M.S., A.S., J.Z., A.B., R.B., D.H., H.L., G.C.R., R.M. and E.G-A. performed the lab-based experiments. R.A, P.M., M.M., V.Z., F.P, M.C., M.R-M. and F.K. performed the physiology experiments. N.H., H.J., L.E.F., P.J.R.B. and T.S., provided gene expression and physiology data. J.W, L.B. and E.P. performed genetic mapping and network studies. X.C., J.X.C., Z.A., M.P. and D.C-D. supervised data analysis and contributed to the experimental design. S.A.C and D.S. planned the experiments. S.A.C. wrote the manuscript with input and discussion from all co-authors.

UKPMC Funders Group Author Manuscript

[14]Cell Signaling & Apoptosis Group at CIBERNED and Vall d'Hebron Institut of Research (VHIR) and Dept Biochemistry-molecular Biology and Institut de Neurociencies at Universitat Autonoma de Barcelona, Barcelona, Spain

[15]Heart Science Centre, National Heart and Lung Institute, Imperial College London, Harefield Hospital, Harefield, Middlesex, UB9 6JH, UK

[16]Cardiovascular Biomedical Research Unit, Royal Brompton and Harefield NHS Trust, Sydney Street, London, SW3 6NP

[17]Department of Epidemiology and Biostatistics, Faculty of Medicine, Imperial College London, Praed Street, London W2 1PG, UK

Abstract

Left ventricular mass (LVM) is a highly heritable trait[1] and an independent risk factor for all-cause mortality[2]. To date, genome-wide association studies (GWASs) have not identified the genetic factors underlying LVM variation[3] and the regulatory mechanisms for blood pressure (BP)-independent cardiac hypertrophy remain poorly understood[4,5]. Unbiased systems-genetics approaches in the rat[6,7] now provide a powerful complementary tool to GWAS and we applied integrative genomics to dissect a highly replicated, BP-independent LVM locus on rat chromosome 3p. We identified endonuclease G (*Endog*), previously implicated in apoptosis[8] but not hypertrophy, as the gene at the locus and demonstrated loss-of-function mutation in *Endog* associated with increased LVM and impaired cardiac function. Inhibition of *Endog* in cultured cardiomyocytes resulted in an increase in cell size and hypertrophic biomarkers in the absence of pro-hypertrophic stimulation. Genome-wide network analysis unexpectedly inferred *ENDOG* in fundamental mitochondrial processes unrelated to apoptosis. We showed direct regulation of *ENDOG* by *ERRα* and *PGC1α*, master regulators of mitochondrial and cardiac function[9,10,11], interaction of ENDOG with the mitochondrial genome and *ENDOG*-mediated regulation of mitochondrial mass. At baseline, *Endog* deleted mouse heart had depleted mitochondria, mitochondrial dysfunction and elevated reactive oxygen species (ROS), which was associated with enlarged and steatotic cardiomyocytes. Our studies establish further the link between mitochondrial dysfunction, ROS and heart disease and demonstrate a new role for *Endog* in maladaptive cardiac hypertrophy.

Elevated left ventricular mass (LVM) is a clinically important trait that independently predicts the risk of heart failure, sudden death and all-cause mortality[2]. Although LVM is a heritable complex trait[1], large genome wide association studies (GWASs) have not identified new LVM genes[3]. Blood pressure (BP)-dependent regulation of LVM, which is perhaps surprisingly limited[7], has been studied extensively in model systems and acts through well-characterised and overlapping signalling modules[12]. In contrast, the pathways underlying BP-independent cardiac hypertrophy, commonly seen in obesity and type 2 diabetes and related to mitochondrial dysfunction and liptoxicity[4,5], remain largely unknown. Here, we took advantage of the recent step-changes in integrative systems-genetics approaches in the rat[6,7] to dissect a BP-independent cardiac mass quantitative trait locus (QTL) and identified the causative gene and underlying mechanism.

The rat is unique for the study of cardiac mass with over 75 QTLs identified for this trait (rat genome database; http://rgd.mcw.edu/). Rat chromosome 3p (0-25Mbp) contains a highly replicated and BP-independent QTL for cardiac mass, which was mapped in crosses of the Spontaneously Hypertensive Rat (SHR) or SHR Stoke Prone (SHRSP) to Wistar Kyoto (WKY) or Salt Sensitive (SS)[13,14]. To dissect genetically this locus, we generated an F_2 intercross from SHR and Brown Norway (BN) strains and replicated further the LVM QTL (LOD=4.2) (Fig. 1a). We confirmed the BP-independent QTL effect in a congenic strain

UKPMC Funders Group Author Manuscript

(SHR.BN-(3L)) that had lower LVM and smaller cardiomyocytes than the SHR (Fig. 1b,c) and refined the QTL region (6.4Mbp-11.2Mpb) using a second congenic strain (SHR.BN-(3S)) (Supplementary Fig. 1). In the F_2 cross, in the SHR.BN-(3L) strain and in previous experimental crosses[13,14], the SHR allele at the locus was associated with increased cardiac mass and this effect was BP-independent (Fig. 1a and d). Functional assessment *in vivo* revealed that the SHR.BN-(3L) strain had better cardiac performance at baseline and following stimulation, as compared to the SHR (Supplementary Fig. 1). These data demonstrate that an SHR allele at the cardiac mass QTL on rat chromosome 3p increases LVM and adversely affects cardiac function.

We used the new genotypes generated in our F_2 cross and those from previous experiments[13,14] to refine the QTL region, and identified five distinct loci (spanning 750kbp in total) that co-segregated with the haplotypes associated with LVM variation (Fig. 1e). *Endonuclease G* (*Endog*), which we had previously shown to be *cis*-regulated in the heart ($P=3\times10^{-6}$)[7], was the only gene at the loci to be differentially regulated with consistent direction of effect in the SHR and SHRSP heart as compared to the WKY heart (Supplementary Table 1). *Endog* is a nuclear-encoded, mitochondrial-localised nuclease with a proposed but disputed function in apoptosis[8,15,16,17] and no known effect on cardiac mass or function. We observed reduced expression of *Endog* transcript and lack of Endog protein in all strains with elevated cardiac mass (Fig. 1f and g). Sequencing of *Endog* revealed promoter and coding sequence variation and we identified an SHR-specific, frameshift-causing insertion in *Endog* exon one that was associated with increased heart weight and LVM (Supplementary Fig. 2). There was marked reduction in cardiac nuclease activity, which was Endog-dependent[18], in SHR heart as compared to BN heart (Fig. 1h and i). In recombinant inbred strains derived from the SHR and BN[6,7] we confirmed the direct relationship between the SHR insertion and the lack of nuclease activity (Fig. 1j) and mapped *Endog*-dependent nuclease activity to a single locus that encodes *Endog* (Fig. 1k) . These data identify *Endog* as the candidate gene at the QTL and infer *Endog* loss-of-function as the mechanism for increased cardiac mass and impaired heart function.

We performed immunoblotting across rat and mouse tissues and determined that Endog was most highly expressed in the heart, localised to cardiomyocytes (Fig. 2) and co-localised with mitochondria (Supplementary Fig. 3). Using short hairpin RNA (shRNA) knockdown of *Endog* (sh*Endog*)[19] we tested the effect of *Endog* loss-of-function in cardiomyocytes and observed an increase in hypertrophic biomarkers and cell size in the absence of pro-hypertrophic stimulation (Fig. 2). Conventional BP-dependent hypertrophic signalling pathways[12] were not activated in sh*Endog* treated cells but we established activation of AMPK (Supplementary Fig. 4), which can induce cardiac hypertrophy[20]. We also observed increased reactive oxygen species (ROS), an additional pro-hypertrophic stimulus[21] that acts through multiple downstream effectors (Supplementary Fig. 4). These data show that *Endog* loss-of-function directly induces cardiac myocyte hypertrophy *in vitro* that is associated with the activation of two pro-hypertrophic pathways both of which have previously been linked with mitochondrial dysfunction[20,21,22].

We then examined the effects of *Endog* loss-of-function *in vivo* in the *Endog* deleted mouse (*Endog*$^{-/-}$)[17] that exhibits no detectable variation in apoptotic phenotypes, an observation that was confirmed in an independent *Endog* deleted strain[16]. As compared to controls, *Endog*$^{-/-}$ mice had larger cardiomyocytes at baseline (Fig. 2) in the absence of stimulation, in keeping with our observations in the SHR.BN-(3L) rat (Fig. 1) and *in vitro* (Fig. 2). Following angiotensin II stimulation of hypertrophy, which is largely ROS-dependent[21], we observed an increase in cardiomyocyte size, hypertrophic biomarkers and LVM in *Endog*$^{-/-}$ mice (Fig. 2 and Supplementary Fig 5). *Endog*$^{-/-}$ mice had BPs equivalent to control mice at baseline (P=0.49) and following angiotensin II stimulation (P=0.51). Our combined *in vitro*

and *in vivo* data confirm a role for *Endog* in cardiomyocyte hypertrophy and identify ROS as a conserved pro-hypertrophic stimulus in both systems.

Endog was proposed[8] but subsequently disputed[16,17] as important for apoptotic cell death and it was unclear how *Endog* loss-of-function was associated with cardiac hypertrophy and dysfunction. To infer *ENDOG* function in the human heart, we carried out genome-wide coexpression network analysis[23] in a large human cardiac expression dataset (n=210) (Supplementary Methods). *ENDOG* was identified in a network that was highly enriched for mitochondrial genes ($P=1.8\times10^{-58}$) and oxidative metabolism processes ($P=4.7\times10^{-38}$) (Fig. 3) (Supplementary Tables 2 and 3). Taken together, the high levels of Endog expression in metabolically active organs (Fig. 2) and in brown fat (Supplementary Fig. 6), the unique co-expression of *ENDOG* with oxidative metabolism genes and the link with AMPK signalling and ROS production pointed to an unappreciated effect of *Endog* in physiological mitochondrial processes.

Peroxisome proliferator activated receptor gamma coactivator 1 alpha (*Pgc1α*) is widely recognised as a master regulator of mitochondrial function[24], and activates many target genes component of the *ENDOG*-associated network (Fig. 3) through interaction with estrogen-related receptor alpha (*Errα*)[9]. Therefore, we tested whether *Pgc1α* also regulated *Endog* and observed robust *Pgc1α*-induced *Endog* transcript and Endog protein expression in cardiomyocytes *in vitro* (Fig. 3). We confirmed the effects of *Pgc1α* variation on Endog protein expression *in vivo* using mice over-expressing *Pgc1α* under the control of muscle creatine kinase (MCK-*Pgc1α*) and in cardiac-specific *Pgc1α* deleted mice ($Pgc1\alpha^{\Delta C/\Delta C}$) (Fig. 3, Supplementary Methods). Luciferase studies revealed strong activation of the *Endog* promoter by *Pgc1α* and *Errα* together (Fig. 3e) and we confirmed direct binding of *ESRRα* to the *ENDOG* promoter by chromatin immuno-precipitation and PCR (ChIP-PCR) in a region containing an *ERRα* response element ($P<0.001$) (Fig. 3f). These data show that *Endog* is a direct target of *ESRRα* and *Pgc1α*, master regulators of mitochondrial and heart function, further inferring a role for *Endog* in mitochondrial and cardiac biology.

It was apparent that the effects of *Endog* loss-of-function on cardiac hypertrophy might be mediated through perturbation of mitochondrial physiology, which we examined. Electron microscopy revealed no gross morphological changes of mitochondria but we observed lipid-like droplets associated with mitochondria from $Endog^{-/-}$ mice that were more numerous and larger than those seen in control mice. Molecular studies revealed marked elevation of triglyceride levels in the $Endog^{-/-}$ mouse heart that was manifest as cardiomyocyte steatosis (Fig. 4 and Supplementary Fig. 7) but not associated with variation in expression levels of fatty acid metabolism or mitochondrial biogenesis genes (Supplementary Fig. 8 and 9). As compared to wildtype littermates, $Endog^{-/-}$ mice had impaired mitochondrial respiration and increased ROS production (Fig. 4).

To assess for mitochondrial depletion we examined mitochondrial DNA (mtDNA)/genomic DNA and mitochondrial protein/tissue weight ratios, which were both diminished in the $Endog^{-/-}$ mouse heart (Fig. 4) in the absence of mtDNA structural variation (Supplementary Fig. 10). This was an intriguing finding given the previously proposed roles for *Endog* in mtDNA synthesis, processing of poly-cistronic mtRNA and mitochondrial biogenesis[25,26] that were subsequently discarded based primarily on experiments in *Endog* deleted mice[16,17]. We re-examined a role of *ENDOG* in mitochondrial biogenesis and demonstrated an increase in mitochondrial mass with chronic *ENDOG* expression in HEK cells ($P<0.01$)and acute *Endog* over-expression in a cardiomyocyte-derived cell line ($P<0.001$) (Fig. 4k-k in the absence of an effect on apoptotic or necrotic cell death (Supplementary Fig. 11). A role for *ENDOG* in mtDNA biology[25,26] was supported further by ChIP-PCR experiments that showed direct binding of ENDOG throughout the mtDNA molecule (Fig.

UKPMC Funders Group Author Manuscript

4n) as previously demonstrated for mitochondrial transcription factor A (TFAM)[27], which is a critical determinant of mtDNA synthesis and repair that when deleted causes eccentric cardiac hypertrophy and heart failure[28].

Mitochondria are essential for oxidative metabolism and mitochondrial dysfunction/ depletion in the heart causes maladaptive cardiac hypertrophy and cardiac dysfunction associated with increased ROS and lipotoxicity[4,5,28,29]. Here we identified *Endog* loss-of-function as a primary determinant of maladaptive cardiac hypertrophy that was associated with mitochondrial dysfunction/depletion and marked cardiomyocyte steatosis. Although the mechanism underlying cardiac hypertrophy due to impaired mitochondrial function is not limited to a single pathway we demonstrated a conserved increase in ROS, an established hypertrophic stimulus[21,22], in *Endog* loss-of-function models. Our studies resolve some of the uncertainty as to the non-apoptotic function of *Endog*[15,16,17] and reveal it's importance in mitochondrial biology, which has intriguing parallels with the dual roles of apoptosis-inducing-factor[30]. We propose that *ENDOG*, which we show binds to mtDNA, modulates mtDNA synthesis, maintenance and/or transcription, in keeping with previous hypotheses[25,26]. Therapeutic targeting the *Pgc1α/Errα* axis has been proposed to improve mitochondrial function in cardiac failure[11] and our studies suggest that regulation of *Endog* is an important component of this process. We conclude that *Endog* is a novel determinant of maladaptive cardiac hypertrophy with previously unappreciated mitochondrial functions.

Methods Summary

Linkage mapping was carried out using microsatellite genotypes in the BNxSHR F_2 population. *Ex vivo* heart weight analysis was performed in the congenic strains, which were characterised using *in vivo* BP telemetry. Comparative haplotype analysis was performed using SNP data (Rat Genome Database; http://rgd.mcw.edu/) for all strains used in the QTL mapping studies. Microarray-based expression analysis was conducted as previously described[6,7]. Cell size and hypertrophy biomarker expression were measured in cardiomyocytes following lentivirus-mediated *Endog* knockdown. Heart weight, hypertrophic biomarker expression and cardiomyocyte cell size were measured in *Endog*$^{-/-}$ mice at baseline and following angiotensin II-induced hypertrophy. Triglyceride abundance, mitochondrial mass and respiratory activity were measured in *Endog*$^{-/-}$ mice as described in the Supplementary material. Weighted gene co-expression network analysis (WGCNA)[23] was applied to the largest publicly available human heart transcriptome dataset. Regulation of *Endog* by *Pgc1α* was investigated in Ad.*Pgc1α*-infected neonatal cardiomyocytes, MCK-*Pgc1* skeletal muscle and *Pgc1* $\alpha^{1C/1C}$ heart samples. ERRα association with the *ENDOG* promoter and *ENDOG*-mtDNA interaction were determined using ChIP. Histological analysis and electron microscopy of *Endog*$^{-/-}$ hearts was carried out to study mitochondrial structure and abundance as well as lipid deposition. MtDNA and gDNA copy number were assessed by QPCR. Mitochondrial abundance was studied in cells by flow cytometry. Full methods are provided in Supplementary Methods.

Supplementary Material

Refer to Web version on PubMed Central for supplementary material.

Acknowledgments

We acknowledge funding from the Medical Research Council (MRC) UK, the National Institute for Health Research (NIHR) UK, the Royal Brompton and Harefield Cardiovascular Biomedical Research Unit, the Imperial College Healthcare Biomedical Research Centre, the British Heart Foundation, the Fondation Leducq, the Wellcome Trust, 301/08/0166 from the Grant Agency of the Czech Republic and 1M0520 from the Ministry of Education of the Czech Republic, PTQ-08-03-07880, SAF2008-02271, SAF2008-03067 and SAF2010-19125 from

the Ministerio de Ciencia e Innovacion (MICINN, Spain), 2009-SGR-346 from the Agència de Gestió d'Ajuts Universitaris i Recerca (AGAUR, Spain), PS09/02034, PS09/01602 and PS09/01591 from Fondo de Investigaciones (FIS, Spain). The European Community's Seventh Framework Programme (FP7/2007-2013) under grant agreement no. HEALTH-F4-2010-241504 (EURATRANS). The German National Genome Research Network (NGFN-Plus) Heart Failure. We thank Dr Michael R. Lieber (University of Southern California) for providing the *Endog* deleted mice and Prof E. Wahle (Institute of Biochemistry and Biotechnology, Halle) for providing the CG4930 expression plasmid. We thank the National BioResource Project-Rat (http://www.anim.med.kyoto-u.ac.jp/NBR/) for providing rat strains.

References

1. Post WS, Larson MG, Myers RH, Galderisi M, Levy D. Heritability of left ventricular mass: the Framingham Heart Study. Hypertension. 1997; 30:1025–1028. [PubMed: 9369250]
2. Lorell BH, Carabello BA. Left ventricular hypertrophy: pathogenesis, detection, and prognosis. Circulation. 2000; 102:470–479. [PubMed: 10908222]
3. Vasan RS, et al. Genetic variants associated with cardiac structure and function: a meta-analysis and replication of genome-wide association data. JAMA. 2009; 302:168–178. [PubMed: 19584346]
4. McGavock JM, Victor RG, Unger RH, Szczepaniak LS. Adiposity of the heart, revisited. Ann Intern Med. 2006; 144:517–524. [PubMed: 16585666]
5. Wong C, Marwick TH. Obesity cardiomyopathy: pathogenesis and pathophysiology. Nat Clin Pract Cardiovasc Med. 2007; 4:436–443. [PubMed: 17653116]
6. Heinig M, et al. A trans-acting locus regulates an anti-viral expression network and type 1 diabetes risk. Nature. 2010; 467:460–464. [PubMed: 20827270]
7. Petretto E, et al. Integrated genomic approaches implicate osteoglycin (Ogn) in the regulation of left ventricular mass. Nat Genet. 2008; 40:546–552. [PubMed: 18443592]
8. Li LY, Luo X, Wang X. Endonuclease G is an apoptotic DNase when released from mitochondria. Nature. 2001; 412:95–99. [PubMed: 11452314]
9. Dufour CR, et al. Genome-wide orchestration of cardiac functions by the orphan nuclear receptors ERRalpha and gamma. Cell Metab. 2007; 5:345–356. [PubMed: 17488637]
10. Wu Z, et al. Mechanisms controlling mitochondrial biogenesis and respiration through the thermogenic coactivator PGC-1. Cell. 1999; 98:115–124. [PubMed: 10412986]
11. Finck BN, Kelly DP. PGC-1 coactivators: inducible regulators of energy metabolism in health and disease. J Clin Invest. 2006; 116:615–622. [PubMed: 16511594]
12. Hill JA, Olson EN. Cardiac plasticity. N Engl J Med. 2008; 358:1370–1380. [PubMed: 18367740]
13. Inomata H, et al. Identification of quantitative trait loci for cardiac hypertrophy in two different strains of the spontaneously hypertensive rat. Hypertens Res. 2005; 28:273–281. [PubMed: 16097372]
14. Siegel AK, et al. Genetic loci contribute to the progression of vascular and cardiac hypertrophy in salt-sensitive spontaneous hypertension. Arterioscler Thromb Vasc Biol. 2003; 23:1211–1217. [PubMed: 12775577]
15. Buttner S, et al. Endonuclease G regulates budding yeast life and death. Mol Cell. 2007; 25:233–246. [PubMed: 17244531]
16. David KK, Sasaki M, Yu SW, Dawson TM, Dawson VL. EndoG is dispensable in embryogenesis and apoptosis. Cell Death Differ. 2006; 13:1147–1155. [PubMed: 16239930]
17. Irvine RA, et al. Generation and characterization of endonuclease G null mice. Mol Cell Biol. 2005; 25:294–302. [PubMed: 15601850]
18. Temme C, et al. The Drosophila melanogaster Gene cg4930 Encodes a High Affinity Inhibitor for Endonuclease G. J Biol Chem. 2009; 284:8337–8348. [PubMed: 19129189]
19. Bahi N, et al. Switch from caspase-dependent to caspase-independent death during heart development: essential role of endonuclease G in ischemia-induced DNA proces sing of differentiated cardiomyocytes. J Biol Chem. 2006; 281:22943–22952. [PubMed: 16754658]
20. Arad M, et al. Constitutively active AMP kinase mutations cause glycogen storage disease mimicking hypertrophic cardiomyopathy. J Clin Invest. 2002; 109:357–362. [PubMed: 11827995]

21. Dai DF, et al. Mitochondrial oxidative stress mediates angiotensin II-induced cardiac hypertrophy and Galphaq overexpression-induced heart failure. Circ Res. 2011; 108:837–846. [PubMed: 21311045]
22. Seddon M, Looi YH, Shah AM. Oxidative stress and redox signalling in cardiac hypertrophy and heart failure. Heart. 2007; 93:903–907. [PubMed: 16670100]
23. Zhang B, Horvath S. A general framework for weighted gene co-expression network analysis. Stat Appl Genet Mol Biol. 2005; 4 Article17.
24. Spiegelman BM. Transcriptional control of mitochondrial energy metabolism through the PGC1 coactivators. Novartis Found Symp. 2007; 287:60–63. discussion 63-69. [PubMed: 18074631]
25. Cote J, Ruiz-Carrillo A. Primers for mitochondrial DNA replication generated by endonuclease G. Science. 1993; 261:765–769. [PubMed: 7688144]
26. Tiranti V, et al. Chromosomal localization of mitochondrial transcription factor A (TCF6), single-stranded DNA-binding protein (SSBP), and endonuclease G (ENDOG), three human housekeeping genes involved in mitochondrial biogenesis. Genomics. 1995; 25:559–564. [PubMed: 7789991]
27. Rothfuss O, et al. Parkin protects mitochondrial genome integrity and supports mitochondrial DNA repair. Hum Mol Genet. 2009; 18:3832–3850. [PubMed: 19617636]
28. Wang J, et al. Dilated cardiomyopathy and atrioventricular conduction blocks induced by heart-specific inactivation of mitochondrial DNA gene expression. Nat Genet. 1999; 21:133–137. [PubMed: 9916807]
29. Lewis W, et al. Decreased mtDNA, oxidative stress, cardiomyopathy, and death from transgenic cardiac targeted human mutant polymerase gamma. Lab Invest. 2007; 87:326–335. [PubMed: 17310215]
30. Vahsen N, et al. AIF deficiency compromises oxidative phosphorylation. EMBO J. 2004; 23:4679–4689. [PubMed: 15526035]

UKPMC Funders Group Author Manuscript

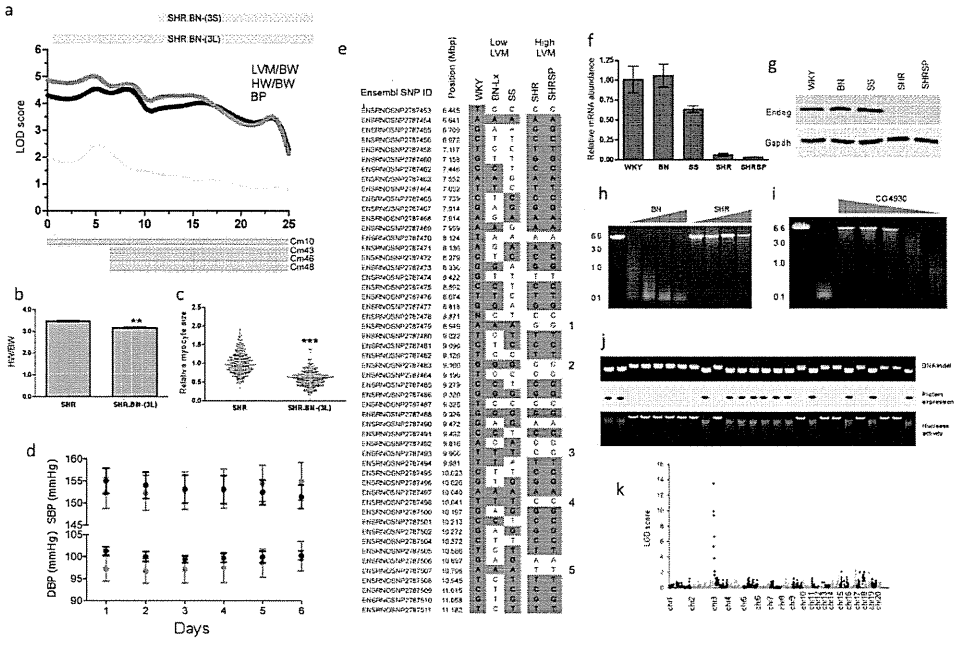

Figure 1. Positional cloning of *Endog* as the gene underlying the rat chromosome 3p cardiac mass quantitative trait locus (QTL)

a, Mapping of heart weight (HW) and left ventricular mass (LVM) corrected for body weight (BW) to chromosome 3p in the Brown Norway (BN) x Spontaneously Hypertensive (SHR) F_2 population. The telomeric limits of the congenic strains (SHR.BN-(3L) and SHR.BN-(3S)) and the previously mapped cardiac mass (CM) QTLs[13,14] are shown; x-axis, physical position in Mbp. **b**, HW indexed to BW in the SHR (n=4) and the SHR.BN-(3L) congenic strains (n=5). **c**, Relative cardiomyocyte cross-sectional area in SHR and SHR.BN-(3L) congenic strains. **d**, *In vivo* telemetric systolic- and diastolic-blood pressure (SBP and DBP) measurements in the SHR (red circles) and SHR.BN-(3L) (black circles) (n=8 per genotype). **e,** Haplotype analysis of the refined QTL region. SNPs are depicted with reference to WKY/NCrl alleles (grey, identical; white, dissimilar) with numbers (1-5) denoting the polymorphic regions between strains with either high or low HW. QPCR of *Endog* mRNA expression (**f**) and immunoblot of Endog protein expression (**g**) in strains with low or high CM at the chromosome 3p locus. **h,** Nuclease activity in BN and SHR heart extracts over a range of cardiac protein extract amounts (grey wedge) (Supplementary Methods). **i**, Reversal of nuclease activity in cardiac lysates by a drosophila-derived inhibitor of Endog[18] (range 1500nM-1.5nM, grey wedge). **j**, Association of the *Endog* indel with loss of Endog protein expression and diminished nuclease activity in the recombinant inbred (RI) strains. Upper, middle and lower panels display the DNA indel, protein expression and nuclease activity, respectively. **k**, Linkage mapping of nuclease activity in RI strains using a quantitative fluorescence-based assay (Supplementary Methods). All data are represented as mean+s.e.m. *, $P<0.05$, **, $P<0.01$, ***, $P<0.001$.